

**FCRD Technical Integration Office (TIO)
DOCUMENT NUMBER REQUEST
TRANSMITTAL SHEET**

1. Document Information

Document Title/Description:	End of Year Status Report on Technical Issues for Transport	Revision:	
Assigned Document Number:	FCRD-USED-2011-000271	Effective Start Date:	September 2, 2011
Document Author/Creator:	B.J. Marshall	OR	
Document Owner:	J.C. Wagner	Date Range:	
Originating Organization:	Oak Ridge National Laboratory	From:	To:
Milestone	<input type="checkbox"/> M1 <input type="checkbox"/> M2 <input checked="" type="checkbox"/> M3 <input type="checkbox"/> M4 <input type="checkbox"/> Not a Milestone		
Milestone Number::	M31UF041203		
Work Package WBS Number:	WP:FTOR11UF0412, WBS 1.02.08.04		
Controlled Unclassified Information (CUI) Type	<input type="checkbox"/> None <input type="checkbox"/> OOU <input type="checkbox"/> AT <input type="checkbox"/> Other		

FCRD	SYSTEM:		
<input type="checkbox"/>	FUEL Advance Fuels		
<input type="checkbox"/>	MPACT Materials Protection, Accounting, and Control for Transmutation		
<input type="checkbox"/>	RES Fuel Resources		
<input type="checkbox"/>	SAFE Regulatory and Safety Crosscut		
<input type="checkbox"/>	SWF Separations and Waste Forms		
<input type="checkbox"/>	SYSA System Analysis		
<input type="checkbox"/>	SYSE System Engineering		
<input type="checkbox"/>	TIO Technical Integration		
<input type="checkbox"/>	TRANS Transmutation Technology		
<input checked="" type="checkbox"/>	UFD Used Fuel Disposition		
<input type="checkbox"/>			
<input type="checkbox"/>	NEAMS Nuclear Energy Advanced Modeling and Simulation		
<input type="checkbox"/>	ODEV Options Development		
<input type="checkbox"/>	REAC Reactor Campaign		

2. Records Management Requirements

Category: General Record QA Record Controlled Doc Controlled QA Doc

Keywords: _____

Medium: Hard Copy CD/Disk (each CD/Disk must have an attached index) Electronic: _____

Total Number of Pages (including transmittal sheet): _____

IF QA Record

QA Classification: Lifetime Non-Permanent

Uniform Filing Code: _____ **Disposition Authority:** _____ **Retention Period:** _____

Special Instructions: _____

3. Signatures

SENDER:			
Robert Howard			02 SEPT 2011
Print/Type Sender Name	Sender Signature		Date
QA RECORD VALIDATOR:			
Print/Type Authenticator Name	Authenticator Signature		Date
ACCEPTANCE/RECEIPT:			
Print/Type Receiver Name	Receiver Signature		Date

Submit to: **Connie.Bates@inl.gov**

 Publication Tracking System

This List: Publication List -

[Publication Tracking System](#) > [Publication List](#)

View Record (Logged in as Weaver, Deborah J)

 [Edit Item](#) |  [Review](#) |  [Change Communication Type](#) |  [Delete Item](#)

Pub ID	31762			
Title	Letter Report - FTOR11UF0412 Transportation - Year-End Report on Technical Issues for Transport			
Status	Submitted for review			
Communication Type	Letter report			
ORNL Review?	Scientific communication that requires ORNL review			
Information Category	Limited By Sponsor			
ORNL Report Classification	Other			
Contact Person	Marshall, William BJ J			
Responsible Organization	Reactor & Nuclear Systems Division (50159781)			
Prepared at	This scientific communication is being prepared by someone at ORNL.			
Authors	Marshall, William BJ J Wagner, John C	ORNL (627296) ORNL (37727)		
Workflow	08/17/2011 17:38:47	Draft	Marshall, William BJ J by Weaver, Deborah J	
	08/19/2011 09:05:09	Author Certification	Marshall, William BJ J	
	08/19/2011 09:05:09	Submitted for review	Marshall, William BJ J	
	08/17/2011 17:38:47	Supervisor	Dunn, Michael E	
	08/25/2011 13:13:46	Technical Reviewer	Scaglione, John M	Auto-Approved Recommended View Comments
	08/26/2011 11:18:27	Technical Reviewer	Howard, Rob L	Recommended View Comments
	08/31/2011 20:43:16	Technical Editor	Harkey, Amy	Recommended View Comments
	09/01/2011 10:32:35	Administrative Check	Weaver, Deborah J	Recommended
		<i>Waiting on the following review(s)</i>		
		Supervisor	Dunn, Michael E	
	Program Manager	Wagner, John C		
	Division Approver	Parks, Cecil V		
	Distributed	Marshall, William BJ J		
Requested Approval Date	August 24, 2011			
Abstract				
Report Number	ORNL/LTR-2011/283			
Secondary ID Number				
Additional Information	This letter report will be transmitted to Paul McConnell, FCT Program UFD Transportation Task Leader, Sandia National Laboratories			
User Facility	Not related to a user facility			
Account Number(s)	35304813			
B&R Codes	AF5865000			
IANs				
FWPs	NEAF346			
Overhead Categories				
Proposal Numbers				
Keywords				

OAK RIDGE NATIONAL LABORATORY

MANAGED BY UT-BATTELLE FOR THE DEPARTMENT OF ENERGY

P.O. Box 2008
Oak Ridge, TN 37831-6170
Tel: (865) 241-3570
Fax: (865) 574-3527
Email: wagnerjc@ornl.gov

Reference: ORNL/LTR-2011/283

September 2, 2011

Mr. Paul McConnell
FCT Program UFD Transportation Task Leader
Sandia National Laboratories
P.O. Box 5800
Albuquerque, New Mexico 87185-0747

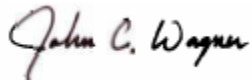
Dear Paul:

End-of-Year Status Report on Technical Issues for Transport – ORNL Fuel Cycle Research and Development (FCR&D) Milestone FCRD-USED-2011-000271 – Due 9/2/2011

This letter documents the completion of the End-of-Year Status Report on Technical Issues for Transport–ORNL Fuel Cycle Research and Development (FCR&D) Milestone FCRD-USED-2011-000271, due September 2, 2011. This report covers work performed during FY11 in support of the Transportation work package (FTOR11UF0412). The enclosed letter report documents work performed for the Used Fuel Disposition Campaign to assess the impact of used nuclear fuel (UNF) degradation and reconfiguration during transportation following extended storage (ES) on criticality safety.

If you have any questions, please contact Rob Howard at (865) 241-5750 or me at (865) 274-1184.

Sincerely,



John C. Wagner, Ph.D.
Reactor and Nuclear Systems Division

JCW:dw

Enclosure

c: R. L. Howard
W. (B.J.) Marshall
J. M. Scaglione
K. Sorenson, SNL

LETTER REPORT

Reactor and Nuclear Systems Division

Project Title: FTOR11UF0412 Transportation

Subject of Document: Year-End Report on Technical Issues for Transport

Type of Document: Letter Report – Assessment of Criticality Safety Impact of Fuel Degradation and Reconfiguration

FCRD Document Identification: FCRD-USED-2011-000271

Authors: William (B.J.) Marshall and John C. Wagner

Date Published: September 2, 2011

Responsible Individuals: John Wagner, ORNL WP Manager
Paul McConnell, UFD WP Manager
John Orchard, DOE WP Manager

Prepared for the
Used Fuel Disposition Campaign
Fuel Cycle Research and Development (FCR&D) Program
Office of Nuclear Energy
U.S. Department of Energy

Prepared by
Oak Ridge National Laboratory
P.O. Box 2008
Oak Ridge, Tennessee 37831-6170
managed by
UT-BATTELLE, LLC
for the
U.S. Department of Energy
under contract DE-AC05-00OR22725

1. INTRODUCTION

This letter report documents work performed for the Used Fuel Disposition Program to assess the impact on criticality safety of used nuclear fuel (UNF) degradation and reconfiguration during transportation following extended storage (ES). This report covers work performed to date during Fiscal Year 2011, from October 1, 2010 through August 31, 2011.

Until a disposition pathway, either recycling or geologic disposal, is chosen and implemented, the storage periods for UNF will likely be longer than were originally intended. Storage periods are uncertain, however 10 CFR 72.42(a) allows an initial license period of up to 40 years and license extensions of up to 40 years. This is combined with the U.S. Nuclear Regulatory Commission (NRC) Waste Confidence Rule (10 CFR 51.23) that states that the Commission has confidence that fuel can be stored safely (wet or dry) for at least 60 years beyond the licensed life of the reactor without significant environmental effects. For a reactor that had an initial operating license of 40 years and was granted a 20-year extension, this means the NRC has confidence that fuel can be stored for a total of up to 120 years. In addition, for its Generic Environmental Impact Statement to support the Waste Confidence Rule, the NRC is analyzing behavior up to 300 years. However, this rulemaking does not grant approval for longer licenses than currently allowed by 10 CFR 72.42(a). Transportation of this UNF following these extended storage periods will still be required to support the ultimate disposition of the material.

A crucial safety issue for transportation following ES is the potential for fuel reconfiguration, which impacts virtually all aspects of a used fuel storage and transport systems' performance, including thermal, shielding, criticality safety, containment, structural performance, and fuel handling and retrievability. The likelihood and potential extent of fuel reconfiguration and the subsequent impact of any reconfiguration on the safety of the UNF are not well understood. Uncertainties related to the mechanical properties of fuel cladding and other structural materials at high burnups (>45 GWd/MTU) exacerbate these concerns. While fuel reconfiguration is of concern both during storage and transportation, this effort is focused primarily on the potential impacts on criticality safety during transportation.

2. BACKGROUND

Fuel reconfiguration has significant safety implications. The focus of this work is to quantify the criticality safety impact of fuel reconfiguration resulting from a loss of fuel integrity. Calculations for used fuel transport cask safety analysis reports (SARs) typically assume as-built fuel assembly geometry. It is therefore essential to determine and understand the potential impacts of fuel reconfiguration on the criticality safety analysis of the storage and transportation casks.

An element of understanding the impacts of long-term storage is related to ensuring that regulatory requirements are maintained. These requirements address key safety-significant aspects of UNF storage and transportation systems, including criticality safety performance and related operational requirements pertaining to UNF handling and retrievability. The appropriateness of the current regulatory requirements over these extended periods will be considered elsewhere. The results of this study can be used to develop an effective approach to address safety, which will also influence, and be influenced by, requirements for retrievability.

The criticality safety requirements for dry storage and transportation of UNF are contained in 10 CFR Parts 72 and 71, respectively [1,2]. The Standard Review Plans [3–5] associated with meeting these regulations are used for guidance in setting target baseline metrics such as the k_{eff} limit of 0.95 for all conditions during storage and transportation. The analyses to be performed as part of this effort can be

used to determine how to integrate the potential impacts of fuel reconfiguration during or following ES on these metrics. The determination of the change in reactivity (Δk_{eff}) caused by scenarios involving such fuel forms or arrangements could be used in at least two different ways. The current k_{eff} limit of 0.95 could be lowered by an identified Δk_{eff} if fuel reconfiguration cannot be precluded. It is also possible that a separate higher limit could be established to allow for the Δk_{eff} margin associated with the worst-case scenarios evaluated in this study. This approach would be similar to the higher limit allowed for the optimum moderation condition applied to dry storage of fresh fuel under 10 CFR 50.68 [6]. In this case, the customary k_{eff} limit would still apply to all conditions involving fuel that had not suffered reconfiguration.

The results of this work may also be used to focus materials research efforts. The scenarios that lead to the highest reactivity increases may be precluded or determined to be incredible with appropriate material information.

Demonstrating compliance with the current confinement requirements contained in Ref. 1 may pose a significant challenge, especially because of the possibility that within the extended time period under consideration, UNF may be transported and then returned to dry storage at another facility. The current requirements include those identified in 10 CFR 72.122(h):

- (1) “The spent fuel cladding must be protected during storage against degradation that leads to gross ruptures or the fuel must be otherwise confined such that degradation of the fuel during storage will not pose operational safety problems with respect to its removal from storage. This may be accomplished by canning of consolidated fuel rods or unconsolidated assemblies or other means as appropriate.”
- (5) “The high-level radioactive waste and reactor-related GTCC waste must be packaged in a manner that allows handling and retrievability without the release of radioactive materials to the environment or radiation exposures in excess of Part 20 limits. The package must be designed to confine the high-level radioactive waste for the duration of the license.”

The overall strategy for this work is to identify scenarios that could result in failure to meet the existing regulations due to ES and high burnup such that appropriate mitigation strategies can be developed to support the technical bases for future licensing efforts.

3. MODELS, CODES, AND METHODS USED

The models, codes, and methods used for these analyses are based on similar work completed previously and documented in Ref. 7. The codes are all part of the Scale code system, documented in Ref. 14.

3.1 CASK MODELS

Three cask models are evaluated: the MPC-24, the GBC-32, and the MPC-68. Each of these models is described in more detail in the following subsections.

All three cask models are based on those used in Ref. 7. The casks are based on the Holtec HI-STAR 100 system and are used here as representative cask models. The incorporation of Holtec designs in this work is not an endorsement of any design or vendor relative to any others.

3.1.1 MPC-24

The MPC-24 cask is designed for the storage and transportation of up to 24 assemblies. The assembly storage cells are separated by flux traps incorporating boron-based poison panels. The fuel assemblies, storage cells, cask basket, poison panels, poison panel wrappers, cask wall, and cask lids are modeled explicitly. The nominal condition for this model is fully flooded with unit density, unborated water. A cross section of the MPC-24 model is shown in Figure 1.

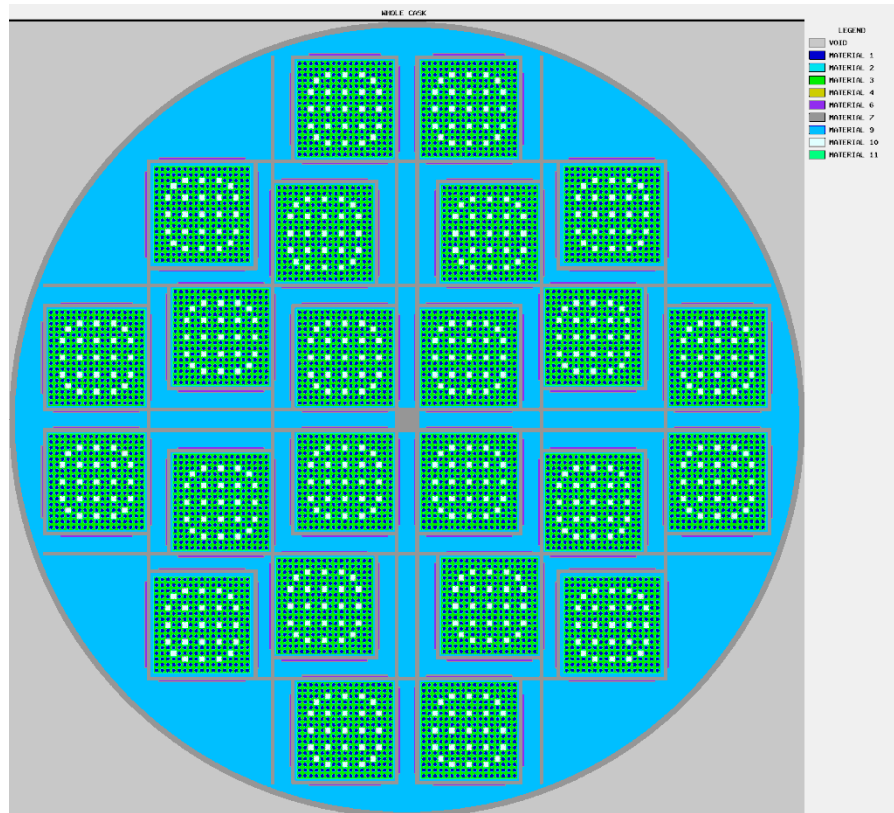


Figure 1. Cross section of MPC-24 model.

Fresh 5 w/o enrichment Westinghouse 17×17 optimized fuel assemblies (OFA) are modeled in the MPC-24. This fuel is used to provide a realistic model that can store high reactivity assemblies. It is unlikely that any fresh fuel assemblies would be placed in ES, but this condition is of interest to complete the parameter space to be covered in this study.

The bottom of the active fuel is modeled as being 10.16 cm (4 in.) above the top surface of the lower cask lid. The top of the active fuel is approximately 77 cm (30.3125 in.) from the bottom surface of the upper cask lid. The volume above and below the active fuel is normally occupied by spacers and fuel assembly hardware, but these are neglected in the model. The spacers are not credited in any fuel reconfiguration scenario, so including them in the model is unnecessary. The impact on calculated k_{eff} should be consistent before and after reconfiguration, so the modeling simplification has no impact on the k_{eff} change calculated in these studies. All fuel assemblies are modeled as nominally centered within the fuel storage cells in the MPC-24 basket.

The storage cell and basket walls are modeled as stainless steel with a thickness of approximately 0.79 cm (5/16 in.). The basket walls are modeled with a height of 448.31 cm (176.5 in.), starting at the upper surface of the bottom cask lid. A gap of approximately 4.60 cm (1 13/16 in.) exists between the top of the basket walls and the lower surface of the upper cask lid. This particular basket configuration consists of 20 standard storage cells with a nominal inner dimension of 22.225 cm (8.75 in.), and four oversized storage cells with a nominal inner dimension of 22.987 cm (9.05 in.). Some design simplifications are incorporated to simplify the computational model. These simplifications are acceptable because they have little to no impact on calculated k_{eff} values and should have no impact on the k_{eff} changes determined in this study.

Two widths of poison panels are used in the MPC-24. The majority of the panels are “wide,” but 16 panels near the periphery of the cask are “narrow” panels. Both panels are modeled with the minimum width of 19.05 cm (7.5 in.) for the wide panels and 15.875 cm (6.25 in.) for the narrow panels. All panels are modeled with a thickness of approximately 0.26 cm (0.101 in.). It is assumed that the entire thickness is poison core; in other words, no face cladding is included in the poison panel models. All poison panels are 396.24 cm (156 in.) in length and are positioned axially 7.3025 cm (2.875 in.) above the upper surface of the lower cask lid. The panels thus overlap the bottom of the active fuel by approximately 2.86 cm (1.125 in.) and overlap the top of the active fuel by approximately 27.6 cm (10.875 in.). The poison loading in the panels is modeled at the minimum specified value of 0.0372 g $^{10}\text{B}/\text{cm}^2$. The poison wrappers are modeled with a nominal thickness of approximately 0.15 cm (0.06 in.). These dimensions are taken from the SAR for the HI-STAR 100 system [8–10].

3.1.2 GBC-32

The GBC-32 model is based on the generic burnup credit storage cask benchmark model defined in Ref. 15. The cask is designed for the storage and transportation of irradiated pressurized water reactor (PWR) fuel assemblies. The details of the cask model are described in Section 2.1 of Ref. 15. The only notable difference from that description is that the top cask lid is 20 cm thick instead of 30 cm. This reduced thickness has no impact on the analyses presented here because the inside cask height is maintained. The reduced steel thickness is therefore on the top side of the top lid, separated from the inside of the cask by 20 cm of steel.

The fuel assemblies, cask basket, poison panels, poison panel wrappers, cask wall, and cask lids are modeled explicitly using half model symmetry. The nominal condition for this model is fully flooded with unit density, unborated water. A cross section of the GBC-32 model is shown in Figure 2.

A range of different initial conditions of fuel assemblies are considered in the GBC-32 models used in these analyses. The representative assembly design is Westinghouse 17×17 OFA at various enrichments, burnups, and cooling times.

The first condition uses the maximum fresh fuel enrichment that can be included in the model to meet a target k_{eff} value of 0.94. The target value of 0.94 is chosen to be less than the regulatory k_{eff} limit of 0.95, to provide some additional allowance for biases and uncertainties that would be included in a safety basis calculation. The maximum fresh enrichment is 1.92 w/o ^{235}U .

The second condition uses the minimum burnup for a 5 w/o initial enrichment assembly that can meet the target k_{eff} value of 0.94 with 5 years of cooling time. The 5 year cooling time period is selected because it is a typical minimum cooling time for a fuel assembly before it can be placed into dry storage. The burnup used for this condition, meeting the target k_{eff} value, is 44,250 MWd/MTU. A series of additional cooling time periods is also analyzed, ranging up to 300 years. Explicit reconfiguration scenario calculations are completed at cooling times of 5, 80, and 300 years.

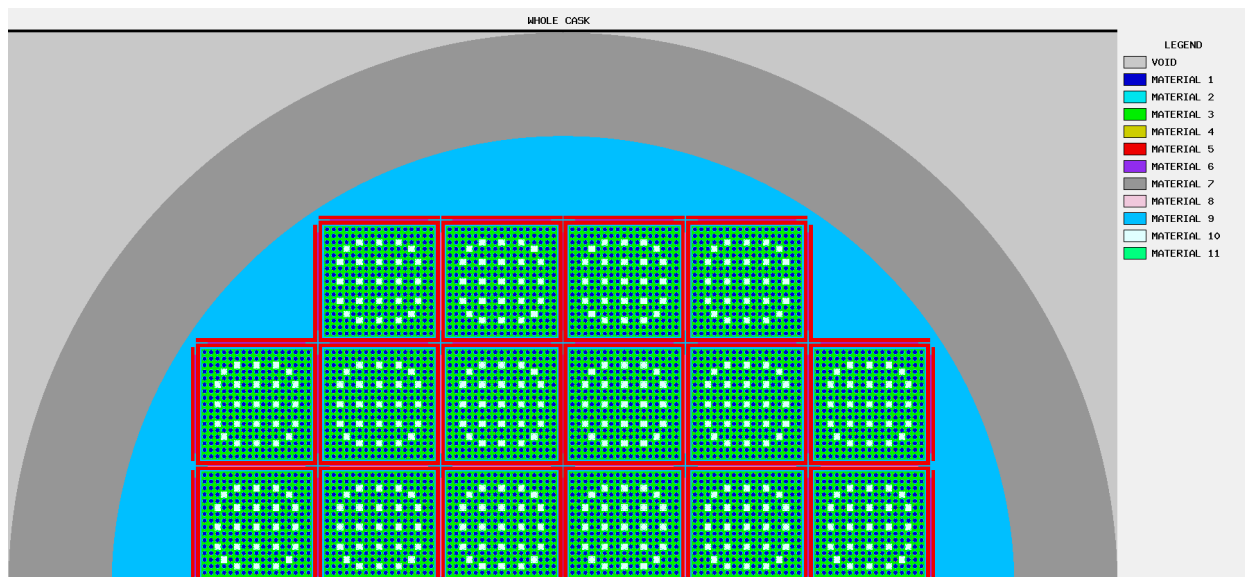


Figure 2. Cross section of GBC-32 model.

The third condition uses a 5 w/o initial enrichment assembly with 70,000 MWd/MTU burnup and 5 years of cooling time. This condition is selected to represent high burnup fuel. A series of additional cooling time periods is analyzed for this burnup as well, ranging up to 300 years. Explicit reconfiguration scenario calculations are also completed at cooling times of 5, 80, and 300 years.

3.1.3 MPC-68

The MPC-68 cask is designed for storage and transportation of fresh BWR fuel assemblies but is being used for evaluating irradiated boiling water reactor (BWR) assemblies. Up to 68 assemblies can be stored in the MPC-68 basket. The assembly storage cells incorporate boron-based poison panels. The fuel assemblies, storage cells, poison panels, poison panel wrappers, cask wall, and cask lids are modeled explicitly. The nominal condition for this model is fully flooded with unit full density, unborated water. A cross section of the MPC-68 model is shown in Figure 3.

The fuel assemblies modeled in the MPC-68 are based on a 10×10 design similar to the GE14 product. For more details about the modeling of the fuel assembly, see Section 3.2.2. The bottom of the active fuel is modeled as being 33.78 cm (~13.3 in.) above the top surface of the lower cask lid. The top of the active fuel is approximately 38.13 cm (~15 in.) from the bottom surface of the upper cask lid. The volume above and below the active fuel is normally occupied by spacers and fuel assembly hardware, but these are neglected in the model. All fuel assemblies are modeled as nominally centered within the fuel storage cells in the MPC-68 basket.

The storage cell and basket walls are modeled as stainless steel with a thickness of 0.635 cm (0.25 in.). The basket walls are modeled with a height of 447.04 cm (176 in.), starting at the upper surface of the bottom cask lid. A gap of 5.87 cm (~2.31 in.) exists between the top of the basket walls and the lower surface of the upper cask lid. The storage cells are modeled with a nominal inner dimension of approximately 15.7 cm (6.18 in.).

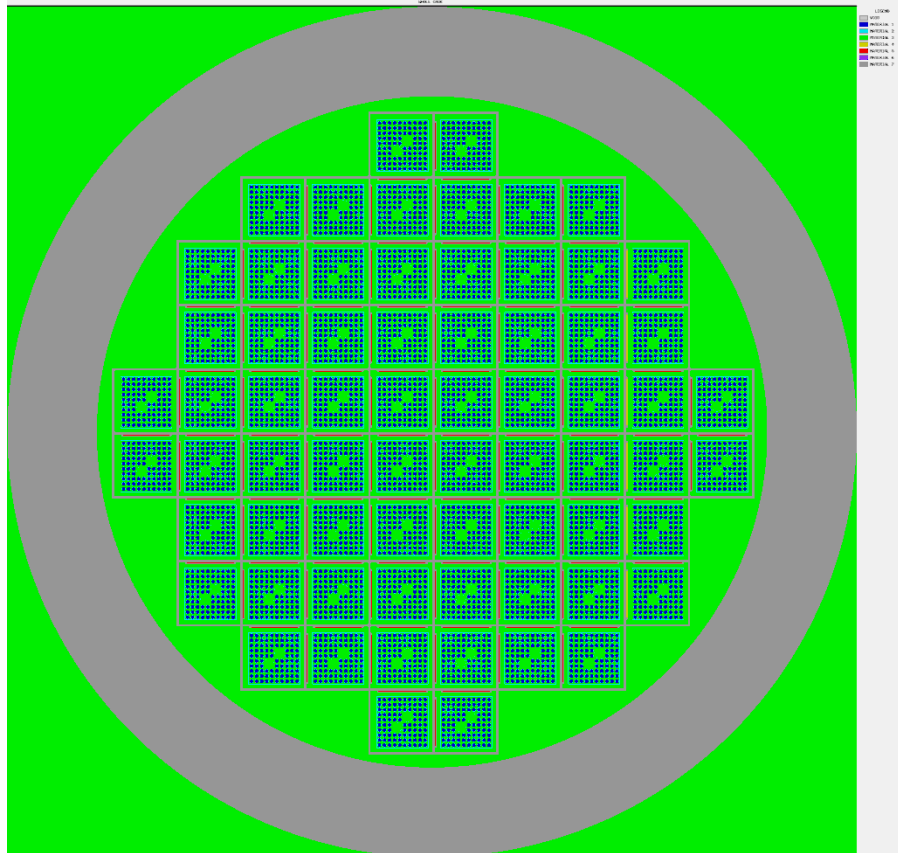


Figure 3. Cross section of MPC-68 model.

The boron-based poison panels are modeled with a width of 12.065 cm (4.75 in.). All panels are modeled with a poison core thickness of 0.2054 cm (0.081 in.). The face cladding is included in the poison panel models with a thickness of 0.0256 cm (0.010 in.). The face clad is modeled as pure aluminum. The total poison panel thickness is 0.2566 cm (0.101 in.) and is modeled centered in a channel with a thickness of 0.2844 cm (0.112 in.). The gaps between the poison panel faces and the poison wrapper walls are filled with water. All poison panels are 393.7 cm (155 in.) in length and are positioned axially 27.43 cm (~10.8 in.) above the upper surface of the lower cask lid. The panels thus overlap the top and bottom of the active fuel by 6.35 cm (2.5 in.). The poison loading in the panels is modeled as $0.0276 \text{ g }^{10}\text{B}/\text{cm}^2$. The poison wrappers are modeled with a nominal thickness of approximately 0.1905 cm (0.075 in.). The dimensions for the MPC-68 models are taken from Ref. 7.

A range of different initial conditions of fuel assemblies are considered in the MPC-68 models used in these analyses. All three conditions use an initial enrichment of 5 w/o ^{235}U and varying burnups and cooling times.

The first condition uses the maximum fresh fuel with an enrichment of 5 w/o. The nominal model k_{eff} value is in excess of 0.96, so this model is not necessarily representative. The lack of axial and radial enrichment zoning, as described in Section 3.2.2, increases the calculated reactivity. A more detailed and realistic model incorporating a maximum enrichment of 5 w/o might be acceptable. An enrichment of approximately 4.36 w/o lowers the calculated k_{eff} to 0.94, which would make the base case reactivity similar to the other conditions discussed below. The effect of this small enrichment variation on the

reactivity changes calculated in the various reconfiguration scenarios would be small and would not impact the k_{eff} change results reported in these analyses.

The second condition uses a 5 w/o initial enrichment assembly with a burnup of 35,000 MWd/MTU and 5 years of cooling time. The burnup used for this condition is chosen to be representative of discharged fuel. The 5 year cooling time period is selected because it is a typical minimum cooling time for a fuel assembly before it can be placed into dry storage. The calculated k_{eff} for this base case is 0.832691 ± 0.000099 . A series of additional cooling time periods is also analyzed, ranging up to 300 years. Explicit reconfiguration scenario calculations are completed at cooling times of 5, 80, and 300 years.

The third condition uses a 5 w/o initial enrichment assembly with 70,000 MWd/MTU burnup and 5 years of cooling time. This condition is selected to be representative of high burnup fuel. The calculated k_{eff} for this base case is 0.767086 ± 0.000099 . A series of additional cooling time periods is analyzed for this burnup as well, ranging up to 300 years. Explicit reconfiguration scenario calculations are also completed at cooling times of 5, 80, and 300 years.

3.2 FUEL ASSEMBLY MODELS

Two fuel assembly designs are used in these analyses: one PWR type and one BWR type. The designs chosen are intended to represent a large portion of the current inventory of discharged UNF as well as a significant portion of the fuel in use currently. The PWR design selected is the Westinghouse 17×17 Optimized Fuel Assembly (OFA). The BWR design selected is a GE 10×10 design based on the GE14 fuel product. Details for the modeling of each assembly type are provided below in separate subsections.

The use of Westinghouse and General Electric fuel assemblies is continued from the work documented in Ref. 7. The use of these fuel types is not an endorsement of any particular fuel design or vendor relative to any others.

3.2.1 Westinghouse 17×17 OFA

Westinghouse 17×17 OFA is a fuel design commonly used in the commercial nuclear industry for the past twenty years. This common use makes it a good choice for a representative fuel assembly type for calculations in the PWR storage and transportation casks. For the purposes of these analyses, the OFA fuel design encompasses all variations of cladding materials, grids, and assembly hardware which may lead to a different fuel product designation from Westinghouse, such as Vantage5 or Vantage+. The essential features are a fuel rod outer diameter of 0.9144 cm (0.360 in.) and a fuel rod pitch of 1.25984 cm (0.496 in).

The 17×17 OFA model included in the MPC-24 and GBC-32 casks contains 264 fuel rods in a square lattice with a center-to-center pitch of approximately 1.26 cm (0.496 in.). The remaining 25 lattice locations consist of 24 RCCA guide tubes and a central instrument tube. The fuel rod array is maintained by these non-fueled locations. The fuel rods are represented with a cold, unirradiated pellet stack height of 365.76 cm (144 in.) and a density of 10.5216 g/cm³, which corresponds to 96% of the theoretical density of UO₂. No density reduction is modeled for pellet dishing or chamfering. The fuel pellet outer diameter is approximately 0.7844 cm (0.3088 in.). The cladding outer diameter is 0.9144 cm (0.360 in.), and the cladding thickness is 0.0571 cm (0.0225 in.). The cladding is modeled as being Zircaloy-4. Unborated, unit density water fills the gap between the pellet and cladding. Water in the pellet/clad gap is conservative for criticality calculations because it causes a slight increase in calculated k_{eff} values. In irradiated fuel, pellet swelling closes this gap and causes this assumption to be nonphysical. A cross section of the 17×17 OFA model is shown in Figure 4.

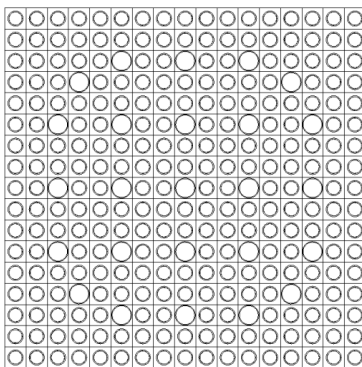


Figure 4. Cross section of 17×17 OFA assembly.

The fuel assemblies are modeled with a uniform initial enrichment in axial and radial directions. No reduced enrichment and/or annular blanket pellets are included in any of the models. No integral burnable absorbers are modeled in the fuel, though the presence of wet annular burnable absorber (WABA) rods is considered during depletion to provide conservative used fuel isotopic compositions with respect to criticality calculations. The details of the depletion conditions are provided in Section 3.4.1.

The guide tube and instrument tubes are assumed to be identical and are represented as Zircaloy-4 with an outer diameter of 1.204 cm (0.474 in.) and a thickness of 0.0407 cm (0.016 in.). The locations within the fuel assembly array can be identified in Figure 4 as the guide tubes are noticeably larger than the fuel rods.

Several modeling simplifications have been incorporated that either have a negligible effect on system reactivity or actually increase assembly reactivity. Some of these simplifications include omission of fuel assembly hardware beyond the ends of the active fuel as well as the omission of all structural and mixing grids, assembly nozzles, plenums, and end plugs. The hardware beyond the active fuel region has a small effect on k_{eff} , and minimal effect on the change in k_{eff} associated with fuel reconfiguration. Omitting the grids allows more effective neutron moderation due to less moderator displacement between rods.

For cases involving depleted fuel, the fuel rods are represented with 18 axial regions. Each region is 20.32 cm (8 in.) tall and contains average mixture number densities in each zone. All fuel rods contain the same composition radially.

3.2.2 General Electric 10×10 BWR Assembly

General Electric 10×10 fuel assembly designs, such as the GE14 fuel product, are widely used in the commercial industry. The 10×10 array is representative of existing BWR fuel assembly designs for use in the MPC-68 cask models.

The GE 10×10 model included in the MPC-68 models contains 92 fuel rods in a square lattice with a center-to-center pitch of 1.295 cm (0.510 in.). The remaining eight lattice locations contain two large water tubes. The fuel rods are represented with a cold, unirradiated pellet stack height of 381 cm (150 in.) and a density of 10.5216 g/cm³, which corresponds to 96% of the theoretical density of UO₂. No density reduction is modeled for pellet dishing or chamfering. The fuel pellet outer diameter is approximately 0.876 cm (0.3449 in.). The cladding outer diameter is 1.026 cm (0.404 in.), and the cladding thickness is 0.066 cm (0.026 in.). The cladding is modeled as being Zircaloy-4. Unborated, unit density water fills the gap between the pellet and cladding. A cross section of the GE 10×10 model is shown in Figure 5.

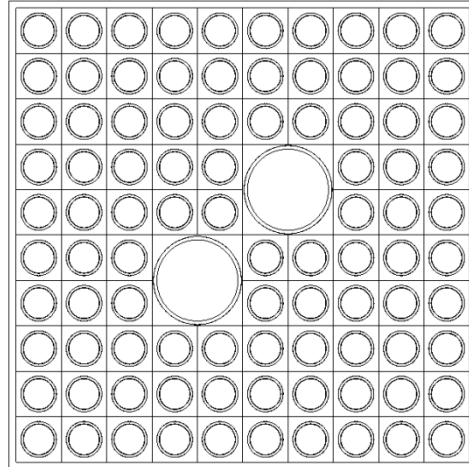


Figure 5. Cross section of GE 10×10 fuel assembly in MPC-68.

The fuel assemblies are considered with a uniform initial enrichment in axial and radial directions. No reduced enrichment axial blanket pellets are included, and no part-length rods are represented in the fuel assemblies. Part length rods are common in BWR assembly designs, including the GE14 design. However, this modeling simplification is expected to provide a conservative estimate for criticality calculations. No burnable absorbers are modeled in the fresh fuel assemblies or during depletion. The impact of burnable absorbers is expected to be negligible on the results of this study. The details of the depletion conditions are provided in Section 3.4.2.

The water tubes are modeled as Zircaloy-4 with an outer diameter of 2.522 cm (0.993 in.) and a thickness of 0.1 cm (~0.039 in.). Each water tube occupies four unit cells in the lattice, displacing a 2×2 region of fuel rods. The water tubes are located near the center of the assembly and are diagonally adjacent to each other. The water rod locations are illustrated in Figure 5.

Several modeling simplifications have been incorporated that either have a negligible effect on system reactivity or actually increase assembly reactivity. Some of these simplifications include omission of fuel assembly hardware beyond the ends of the active fuel as well as the omission of all structural and mixing grids, assembly end fittings, plenums, and end plugs. The hardware beyond the active fuel region has a small effect on k_{eff} , and minimal effect on the change in k_{eff} associated with fuel reconfiguration. Omitting the grids allows more effective neutron moderation due to less moderator displacement between rods.

For cases involving depleted fuel, the fuel rods are represented with 25 axial regions. Each region is 15.24 cm (6 in.) tall and contains average mixture number densities in each zone. All fuel rods contain the same composition radially.

3.3 SOFTWARE CODES

These analyses require a large number of k_{eff} calculations and also require some depletion calculations to generate used fuel isotopic number densities. The SCALE code system was used to perform various types of calculations. The KENO-V.a and KENO-VI Monte Carlo codes are used for k_{eff} calculations. All depleted fuel isotopic compositions were generated with either the TRITON t-depl sequence or the STARBUCS sequence. KENO-V.a and KENO-VI are documented in Sections F11 and F17, respectively, of Ref. 14. The TRITON and STARBUCS sequences are documented in Sections T01 and

C10, respectively, of Ref. 14. Descriptions of each of these codes and some discussion of their methodologies are provided in the subsections below.

3.3.1 KENO Monte Carlo Codes

The KENO-V.a and KENO-VI Monte Carlo codes are both used in these analyses. Both codes use similar tracking algorithms, cross section processing, and material descriptions. KENO-V.a has a more restrictive geometry package that is useful for most simple configurations and executes relatively quickly. KENO-VI contains a general geometry package and can model a broader range of configurations than KENO-V.a. KENO-VI runs significantly more slowly than KENO-V.a and is therefore used only when necessary. The majority of the cases run for these analyses used KENO-V.a. A base case model is constructed in both codes for the appropriate and consistent calculation of reactivity effects in each of the reconfiguration scenarios.

The KENO codes are executed within the SCALE system using the CSAS5 or CSAS6 sequences. The CSAS sequences execute the appropriate codes (BONAMI, WORKER, CENTRM, and PMC) to generate a set of problem-dependent, resonance-corrected cross sections and then use those cross sections in a 3-dimensional Monte Carlo simulation to determine the k_{eff} for the desired model. For these analyses, all cases were run with the 238-energy-group ENDF/B-VII.0 library distributed with SCALE.

3.3.2 TRITON Depletion Sequence

The TRITON control module was used in these analyses to generate ARP libraries representing the fuel types modeled with depletion desired parameters. To do this, the t-depl sequence is executed to run a series of NEWT cases to obtain detailed flux solutions that are used in multiple ORIGEN-S depletion calculations to calculate burned fuel isotopic compositions.

NEWT performs a 2-D deterministic transport calculation to generate the fluxes that are used in the ORIGEN depletion. The 2-D model used in NEWT is essentially a slice through the 17×17 OFA or GE 10×10 assemblies described above in Sections 3.2.1 and 3.2.2.

ORIGEN-S generates time-dependent isotopic number densities for a large number of isotopes as they are generated and/or depleted through fission, transmutation, and decay. The detailed calculations performed by ORIGEN are retained in libraries so that the ORIGEN-ARP process can regenerate the number densities with high fidelity through interpolation among the known state points analyzed explicitly in TRITON. The ORIGEN-ARP approach is used in STARBUCS, discussed in Section 3.3.3, to generate depleted isotopic number densities much more quickly than is possible with multiple TRITON runs. The ORIGEN-ARP methodology can be used when the underlying libraries are generated with the same depletion parameters of interest. The depletion parameters used in these analyses are discussed for PWR fuel in Section 3.4.1 and for BWR fuel in Section 3.4.2.

3.3.3 STARBUCS and ORIGEN-ARP

The STARBUCS sequence within SCALE can be used to perform depletion calculations via the ORIGEN-ARP methodology. The depleted isotopic compositions are then integrated into a provided KENO model for the calculation of k_{eff} values. The depletion inputs needed are fairly simple and consist of a fresh fuel composition, an irradiation history, and an ARP library or libraries. The results can be further tailored by providing parameters to model axial burnup and moderator density profiles, the isotopes to retain in the KENO calculations, and post-discharge cooling time.

The ORIGEN-ARP methodology performs depletion calculations with much greater speed than TRITON by interpolating on cross sections stored in the data libraries created by TRITON. The cross section interpolation algorithm allows rapid calculations to any point within the covered phase space with virtually no sacrifice in accuracy. The ARP libraries generated by TRITON must cover the entire desired parameter range as extrapolation is not allowed. For example, explicit TRITON calculations with initial enrichments of 3 w/o and 5 w/o would allow depletion calculations for any initial enrichment in the range of 3 to 5 w/o, inclusive. Similarly, the libraries must bound the intended burnup range of subsequent depletion calculations. This approach allows for the efficient generation of a large number of depleted fuel compositions with a relative small number of computationally intensive TRITON calculations.

3.4 DEPLETION CONDITIONS

In all burnup credit analyses, the depletion conditions that the fuel experiences can have a significant impact on the calculated k_{eff} values. In these analyses, the depletion conditions are intended to be representative of conditions that would be used in a burnup credit analysis but are not intended to be particularly conservative or bounding. Generic data is used in the PWR depletion conditions as PWR burnup credit has been studied extensively. The BWR depletion conditions are more representative and are based on the operating history of a specific assembly.

Several key factors can impact the reactivity of discharged fuel in LWR burnup credit. The key parameters include the nuclides represented in the isotopic compositions, parameters used for the depletion analysis, cooling time, axial burnup profiles, and horizontal burnup profiles. A listing of important burnup credit parameters is provided in Ref. 16.

The depletion calculations performed for these analyses for both BWR and PWR fuel consider the same isotopes. The isotopes considered are shown in Table 1. The nuclides considered include 12 actinides (isotopes of uranium, plutonium, americium, and neptunium) and 16 fission product isotopes. The list of isotopes is taken from Ref. 17 and is listed as Set 2 in Table 1 of the reference. Although Ref. 17 specifically addresses PWR burnup credit, the major isotopes effecting reactivity of irradiated uranium oxide fuel will be the same in BWR fuel.

A range of post-irradiation cooling times is considered in these analyses for both PWR and BWR fuel. Reference 17 provides details on the reactivity changes experienced by used fuel as a function of time since discharge. For the “Set 2” isotopes considered in these analyses, the reactivity of the depleted fuel decreases fairly steadily between 5 and about 100 years after discharge. The primary decays that drive this change are the ^{241}Pu into ^{241}Am (14.4 year half-life) and ^{155}Eu into ^{155}Gd (4.7 year half-life). Beyond about 100 years after discharge, the reactivity of the fuel increases primarily due to the decay of ^{241}Am (433 year half-life) and ^{240}Pu (6560 year half-life). This increase continues until about 20,000 years after discharge, which is dependent upon enrichment, burnup, and service history. A plot for PWR fuel is shown in Figure 6 and is expected to be similar for BWR fuel as well. Note that the maximum reactivity of used fuel considering “Set 2” isotopes occurs at discharge, and the reactivity after 5 years of cooling time is higher than the subsequent local maximum around 20,000 years later. These analyses considered cooling times ranging from 5 years to 300 years, with explicit reconfiguration scenario calculations at cooling times of 5, 80, and 300 years. The effects of cooling time on the various reconfiguration scenarios are considered, and they are discussed in Section 5.

Table 1. Isotopes included in depleted fuel models

Actinides					
²³⁴ U	²³⁵ U	²³⁶ U	²³⁸ U	²³⁸ Pu	²³⁹ Pu
²⁴⁰ Pu	²⁴¹ Pu	²⁴² Pu	²⁴¹ Am	²⁴³ Am	²³⁷ Np
Fission products					
⁹⁵ Mo	⁹⁹ Tc	¹⁰¹ Ru	¹⁰³ Rh	¹⁰⁹ Ag	¹³³ Cs
¹⁴³ Nd	¹⁴⁵ Nd	¹⁴⁷ Sm	¹⁴⁹ Sm	¹⁵⁰ Sm	¹⁵⁰ Sm
¹⁵² Sm	¹⁵¹ Eu	¹⁵³ Eu	¹⁵⁵ Gd		

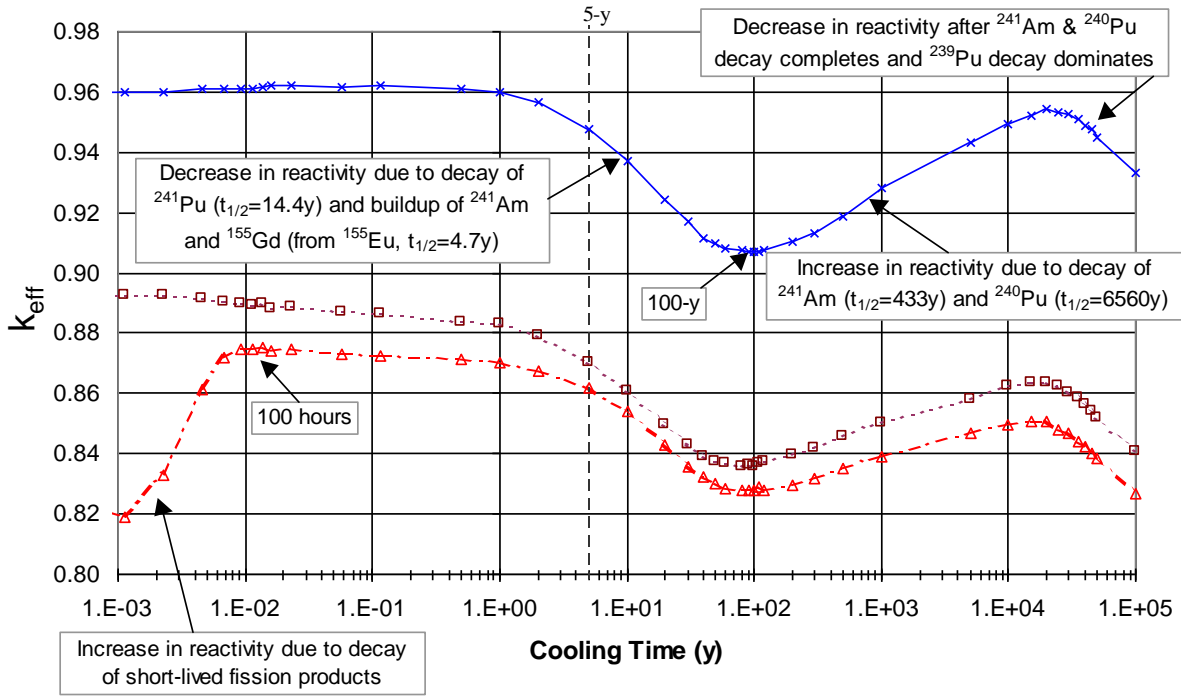


Figure 6. Reactivity behavior of fuel with cooling time in a GBC-32 cask (4.0 wt% 40 GWd/MTU burnup).

In the analyses performed here, the radial burnup profile is assumed to be uniform. The primary focus of this study is reactivity change for different geometry scenarios, so neglecting radial burnup effects is acceptable because any potential change in absolute reactivity caused by such detail is likely to be consistent in when determining the change in calculated k_{eff} .

More details regarding the parameters used for the depletion analysis and axial burnup profiles for both PWR and BWR cases are provided in the subsequent subsections.

3.4.1 PWR Depletion Conditions

The depletion parameters that impact discharged fuel reactivity as listed in Ref. 16 are fuel temperature, moderator temperature/density, soluble boron concentration, specific power and operating history, use of burnable poisons, and use of integral burnable poisons. Each of these parameters must be addressed in a burnup credit analysis to demonstrate that conservative depletion parameters have been implemented in

the safety basis. These depletion calculations are intended to provide used fuel isotopic compositions that are representative of the compositions generated for a safety analysis.

The temperature of the fuel during depletion is important to discharged reactivity because it can cause a hardening of the neutron spectrum during depletion. The higher population of fast neutrons will generate more plutonium via an increased number of parasitic neutron captures in ^{238}U . The resonance absorption in ^{238}U is increased at elevated fuel temperatures. Higher fuel temperatures are therefore considered conservative, with 1000 K suggested as a possible value in Ref. 16. The fuel temperature used in the TRITON models was 1100 K.

The moderator temperature and density also affect depleted fuel reactivity by directly impacting the thermalization of the neutron spectrum. As mentioned above, a harder neutron spectrum will result in increased plutonium production and correspondingly higher reactivity in the depleted fuel. For PWR cores, the reactor coolant system pressure is held constant but the coolant temperature will change the moderator density. A moderator temperature of 600 K is postulated in Ref. 16 as a potentially acceptable value for use in PWR burnup credit applications. In the TRITON depletion calculations used in this study, a moderator temperature of 610 K with a corresponding moderator density of 0.63 g/cm^3 was used. This temperature and density combination is used at all axial elevations in the fuel assembly.

Soluble boron is used for fine reactivity control during PWR operations and is primarily adjusted to offset depletion effects. The soluble boron concentration may increase early in a cycle if burnable absorbers are present and deplete quickly enough. This is the typical behavior for Westinghouse plants using the Integral Fuel Burnable Absorber (IFBA) as the primary burnable absorber. Cores using other burnable absorbers will tend to see a monotonically decreasing soluble boron concentration, though the rate of decrease may vary as a function of depletion. The effect of the soluble boron is similar to the effect of moderator density in that the presence of boron directly causes a spectral shift. In this case, higher soluble boron concentrations increase discharged fuel reactivity by reducing the population of thermal neutrons and hardening the spectrum. The typical practice in PWR burnup credit applications is to use a constant soluble boron concentration that is higher than the assembly life-cycle average, thus conservatively exposing the fuel to a faster spectrum than it would actually experience for at least the majority of its depletion. The average soluble boron concentration for PWR plants operating in the United States today is on the order of 800–900 ppm, so a concentration of 1000 ppm is frequently used as the bounding constant value. The TRITON calculations supporting this analysis used a constant soluble boron concentration of 1000 ppm.

The specific power and operating history experienced by fuel during depletion have been shown in some studies to impact the discharged fuel reactivity. The effect is typically small and varies considerably depending on the set of isotopes used in modeling the UNF. For this reason, Ref. 16 recommends using a best estimate value for the specific power and a constant full power during depletion calculations. It further recommends that an additional uncertainty be used to account for the deviation of actual depletion conditions from those considered in the analysis. A specific power of 60 MW/MTU was used for these depletion calculations. This specific power is too high for typical PWR operations, but it is acceptable because of the small sensitivity of the discharged reactivity to the selected specific power level.

Fixed burnable poisons are burnable poisons that are placed in a constant location inside a fuel assembly for the duration of the cycle but are not mixed with or applied to the fuel pellets. In Westinghouse plants, these absorbers are typically placed within the guide tubes in assemblies that are not positioned under RCCAs. Historically, borosilicate glass rods were used, but more recently Wet Annular Burnable Absorber (WABA) rods have been used. Many plants have completely abandoned the use of fixed burnable poisons. The reactivity effects for these poisons typically are twofold: the boron-based poison hardens the spectrum by selective absorption of low energy neutrons, and the water displacement within

the guide tubes decreases moderation. Both of these cause spectral hardening and increased reactivity in depleted fuel. Reference 18 studied the impact of a range of fixed burnable poisons in Westinghouse designs and determined that longer exposure times and a larger number of rods both increased the impact of the fixed poisons. For that reason, 24 WABA rods are present for the entire depletion. The maximum number of WABA rods that can be used is 24 as there are 24 guide tubes in 17×17 OFA assemblies. WABA are typically used only during the first cycle of operation, but sometimes they are used for a second cycle. Using the fixed poison for the entire depletion is therefore bounding of actual operation with respect to discharge reactivity effects. The poison composition within the WABA rods is depleted during the TRITON calculations.

The axial burnup profile can have a significant effect on discharged assembly reactivity. The impact of the axial profile is a balance between the higher relative burnup in the middle elevations of the assembly and the higher leakage at the ends of the assembly. Once the burnup difference between the central and the end regions of the assembly is great enough, the additional neutron leakage effect from the end is overcome. In this condition, the reactivity of the assembly is highly sensitive to the reactivity of the end of the assembly and its low relative burnup. The top end of the assembly tends to be more limiting than the bottom end for two reasons, both related to the moderator temperature and density profile. In commercial power reactors, the coolant flow is from the bottom to the top of the core. The colder water at the bottom of the core is denser and is more effective at thermalizing neutrons. This leads to a slight increase in relative burnup compared to the top end of the assembly, and the softer spectrum produces somewhat less plutonium near the bottom end. The burnup at which this distributed burnup profile becomes limiting and the magnitude of the reactivity end-effect can be a function of burnup, initial enrichment, and axial profile. At the burnups of typical discharged PWR fuel (i.e., burnups greater than about 30 GWd/MTU), the distributed profile will be more limiting than a uniform profile.

A set of limiting burnup profiles as a function of assembly burnup has been generated for PWR fuels in Ref. 11 from a database of axial burnup profiles [20] for fuel assemblies with no axial zoning. The bounding 18-zone profiles identified in Ref. 11 are available as default burnup profiles in STARBUCS. These default profiles were used in these analyses. The STARBUCS depletion assumes the relative burnups of the discharged fuel are constant in each zone for the entire depletion. In other words, the discharged relative burnup profile is held as a constant power profile throughout the depletion. The depletion calculations performed to 44,250 MWd/MTU used Profile 2 from Table 5 in Ref. 11, while the depletion calculations performed to 70,000 MWd/MTU used Profile 1 from the same source. The use of these profiles is appropriate since no axial zoning features are modeled in the PWR fuel, as discussed above in Section 3.2.1.

3.4.2 BWR Depletion Conditions

The mechanisms whereby depletion conditions influence discharge fuel assembly reactivity are largely similar for BWR and PWR fuel. The detailed discussion from Section 3.4.1 therefore does not need to be repeated here. Less generic work has been documented regarding BWR burnup credit, so this section will focus more on the development of the depletion conditions that were used. Data for specific BWR assemblies is therefore gathered and reviewed from the commercial reactor critical (CRC) state points documented in Refs. 12 and 13. The details of how this information is used are provided here.

It is assumed that the effects described above for PWR depletion conditions have similar impacts for BWR burnup credit, though in many cases explicit studies to demonstrate this have not been performed. Since the effects of the various depletion conditions are believed to be well understood, however, this is a relatively safe assumption for the simple fuel assembly design considered in these analyses.

The fuel temperature used in the BWR depletions is 840 K.

The impact of moderator temperature and density in a BWR is driven mostly by the void history of an assembly. The void fraction in each axial node for each assembly is provided in the CRC state point data in Refs. 12 and 13. From these data it is possible to generate an average void fraction for each node in an assembly. The average void history for each node can then be input to STARBUCS and used to generate more representative UNF compositions. The average void values are determined for assembly C30 from LaSalle Unit 1 Cycles 5–7. This assembly is selected based on a limiting burnup profile, as discussed below. The void fractions for each elevation as a function of burnup are provided in Ref. 13, and the average void fractions used are shown in Table 2.

Table 2. Average moderator density by axial node, based on assembly C30 from LaSalle Unit 1

Axial zone midpoint elevation (cm)	Average moderator density (g/cm³)	Axial zone midpoint elevation (cm)	Average moderator density (g/cm³)
7.62	0.7396	205.74	0.3126
22.86	0.7396	220.98	0.2953
38.10	0.7288	236.22	0.2802
53.34	0.6875	251.46	0.2668
68.58	0.6349	266.70	0.2549
83.82	0.5798	281.94	0.2445
99.06	0.5284	297.18	0.2354
114.30	0.4831	312.42	0.2276
129.54	0.4434	327.66	0.2213
144.78	0.4089	342.90	0.2163
160.02	0.3794	358.14	0.2128
175.26	0.3539	373.38	0.2115
190.50	0.3317		

Each ARP library generated in TRITON represents a single 2-D slice through the assembly. It is therefore necessary to generate a range of libraries covering all possible moderator densities for use in STARBUCS. Based on the range of average densities provided in Table 2, ARP libraries are generated with densities from 0.2 g/cm³ to 0.8 g/cm³ with intervals of 0.1 g/cm³. STARBUCS is able to interpolate the appropriate cross section data for the specific void fractions in Table 2 within the generated moderator density points.

Soluble boron is not used in commercial BWR operations. It is therefore not necessary to model the presence of soluble boron during depletion for BWR fuel.

Discharged assembly reactivity is not highly sensitive to operating history or specific power. The depletion calculations for these analyses model a specific assembly, C30, from a specific commercial BWR plant, LaSalle Unit 1. The specific power can be estimated from data provided in Ref. 13. The core power, number of assemblies, and MTU loading per assembly can be used to determine the average specific power in MW/MTU (W/g). The average burnup of the assembly compared to the cycle burnup can be determined for each data point, and thus a relative power can be calculated. The burnup-weighted average specific power for assembly C30 is slightly greater than 30 MW/MTU. This value is used in the TRITON depletion calculations to generate the ARP libraries for the STARBUCS calculations. Both calculations assume a constant, full power operating history. These assumptions are accurate enough to provide realistic estimates of the UNF reactivity.

BWR fuel assemblies are typically operated for a portion of their life cycle with control blades inserted. The BWR control blades are external to the assembly itself but adjacent to two faces of the assembly channel. This operating strategy is analogous in many ways to the use of fixed poisons in PWR plants in relation to the impact of discharged fuel reactivity. The impact of control blade presence in such a fashion is neglected in these analyses. The absolute reactivity would be increased if rodded operations were considered, but the effect on the reconfiguration scenario reactivity consequence is expected to be negligible.

BWR fuel assemblies typically contain some fuel rods with Gd_2O_3 present as a burnable poison. The presence of these rods can cause reactivity to increase as a function of depletion early in life because the Gd_2O_3 depletes more quickly than the ^{235}U . The reactivity of the assembly typically peaks and starts to decrease after assembly burnups of 9–12 GWd/MTU. This maximum reactivity point has historically been the primary interest of BWR spent fuel pool criticality safety analyses. The analyses for this report are based on an assumption of crediting burnup beyond this peak and consider the reactivity of the fuel at typical discharge burnups of 35 GWd/MTU and a high burnup of 70 GWd/MTU. The peak reactivity point is therefore of little interest. The presence of gadolinia absorbers is therefore neglected in both the fresh and used fuel compositions. The change in k_{eff} will be consistent before and after reconfiguration and is therefore not relevant to this study.

As discussed above in Section 3.4.1, the axial burnup profile modeled impacts the calculated reactivity of UNF. The gradient at the top end of the fuel assembly is the most important feature in driving reactivity in one profile relative to another. It is expected that BWR profiles are more severe than PWR profiles because the top of the assemblies often experience high void fractions. This high void fraction and corresponding lack of moderation leads to lower relative burnups in the top section of a BWR assembly than a PWR assembly. The low burnup region will also have a relative increase in plutonium generation. For these reasons, the axial burnup profiles in the PWR database [20] cannot be used for BWR fuel. No analogous database of BWR axial burnup profiles exists, so axial burnup profiles from the CRC data for Quad Cities Unit 2 [12] and LaSalle Unit 1 [13] are surveyed for profile selection.

The relative burnup profiles for all assemblies presented in Refs. 12 and 13 are generated and compared to determine a potentially limiting burnup profile for use in these analyses. The two plants have different active fuel heights, so a candidate is first selected from each plant, and then the two potentially limiting profiles are compared to select the profile for use in these calculations. The relative burnup profiles are compared based on the integral relative burnup over two different axial extents from the top of the assembly. The relative burnups of the top 3 and top 6 nodes are summed, with lower sums indicating lower relative burnup and higher reactivity. For Quad Cities Unit 2, assembly E7 has the lowest relative burnup in the top 3 nodes, but assembly F8 has the lowest relative burnup over the top 6 nodes. Assembly C30 has the lowest relative burnup over both 3 and 6 nodes for all the assemblies considered from LaSalle Unit 1. The relative burnup profile for assembly C30 is more severe over both the top 3 nodes and top 6 nodes than either E7 or F8 from Quad Cities Unit 2. The three potential profiles, including the integrated relative burnup over the top 3 and top 6 nodes, are provided in Table 3. The LaSalle fuel has an active length of 150 in., compared to the 144-in. active length of fuel used at Quad Cities. This difference in length is not expected to cause a significant difference in calculated reactivity, so the use of LaSalle Unit 1 fuel is acceptable for these calculations. A comprehensive study would be required to identify a limiting axial burnup profile for BWR fuel. The profile used here is similar to, though not as extreme as, a potentially limiting profile identified in Ref. 22. The lower gradient used in this analysis is not expected to have a significant impact on the calculated change in k_{eff} caused by fuel reconfiguration.

Table 3. Potentially limiting relative burnup profiles from Quad Cities Unit 2 and LaSalle Unit 1

Axial zone midpoint elevation (cm)	Assembly 30 (LS U1)	Assembly E7 (QC U2)	Assembly F8 (QC U2)
7.62	0.2461	0.2141	0.2228
22.86	0.7879	0.7470	0.7500
38.10	1.0175	0.9788	0.9813
53.34	1.1026	1.0980	1.0996
68.58	1.1751	1.1518	1.1568
83.82	1.1942	1.1781	1.1877
99.06	1.2052	1.1967	1.2087
114.30	1.2168	1.2125	1.2270
129.54	1.2481	1.2522	1.2668
144.78	1.2535	1.2602	1.2743
160.02	1.2526	1.2589	1.2734
175.26	1.2485	1.2523	1.2657
190.50	1.2419	1.2458	1.2531
205.74	1.2320	1.2391	1.2361
220.98	1.2170	1.2306	1.2139
236.22	1.1955	1.2084	1.1843
251.46	1.1655	1.1651	1.1412
266.70	1.1260	1.1165	1.0940
281.94	1.0759	1.0555	1.0358
297.18	1.0118	0.9569	0.9425
312.42	0.9112	0.8369	0.8270
327.66	0.7873	0.6815	0.6773
342.90	0.6336	0.2968	0.3065
358.14	0.2886	0.1662	0.1742
373.38	0.1656		Not Applicable
Top 3 Nodes	1.0878	1.1446	1.1580
Top 6 Nodes	3.7980	3.9939	3.9633

4. RECONFIGURATION SCENARIOS CONSIDERED

This section of the report describes the reconfiguration scenarios considered in these analyses. These scenarios do not represent the results of specific reconfiguration progressions; rather they are designed to be of any reconfiguration conditions that could occur. It is realized that a number of intermediate variations and different combinations of variations are possible, but the selected scenarios will identify which should be explored in more detail and which can be discounted from further consideration. The conditions included in the models are described below.

4.1 FUEL ROD COLLAPSE

The collapse of a fuel rod is hypothesized to result from the failure of fuel rod cladding. The collapse could be the result of a static or dynamic load if the material properties have changed sufficiently after extended time periods. Scenarios involving both single and multiple rod failures are included and discussed in more detail below.

4.1.1 Single Rod Failure

The single rod failure scenario is predicated on the collapse of an entire fuel rod due to cladding failure. The fuel and cladding material would fall to the bottom of the cask, thus leaving an empty location in the lattice. In many internal locations within a fuel assembly lattice, this results in an increase in reactivity in the fully flooded condition due to increased moderation. The collapsed rod itself is not modeled as rubble on the bottom of the cask. The fissile material would form a fairly thin, severely undermoderated heap below the fuel assembly. This rubble would have much lower reactivity than the assembly itself.

Each unique rod location is assumed to have collapsed for both the PWR and BWR fuel assemblies. The assembly and cask symmetry and asymmetry are accounted for in the determination of unique locations, with possible exceptions for peripheral storage locations. The BWR assembly in the most common storage cell is half-assembly symmetric, with the line of symmetry running diagonally from the northwest to southeast corners as seen in Figure 5. The PWR assembly is eighth-assembly symmetric. In all three cask designs, all assemblies in the cask are assumed to have the same fuel rod collapse.

4.1.2 Multiple Rod Failure

The multiple rod failure scenarios are based on the assumption that multiple rod failures can occur if a single rod collapse is credible. As with the single rod failure scenario, the material from the collapsed rods falls to the bottom of the cask, leaving empty locations within the fuel assembly lattice. Rods are removed in small groups until an optimum reactivity is achieved. Also as with the single rod failure cases, the debris at the bottom of the cask is not modeled. For the larger number of rods removed to achieve optimum reactivity, this assumption is likely conservative as a significant amount of debris material will be accumulating within the assembly storage cell. All fuel assemblies are assumed to have the same set of rods collapse.

The results of the single rod failure scenarios are used to generate likely limiting scenarios for small numbers of rods removed. As additional rods are removed in each step, a series of potentially limiting configurations is generated to determine the most reactive configuration with a given number of rods removed. In most cases, the potentially limiting configurations for a given number of removed rods are generated from previous configurations that were not limiting as well as from the limiting configuration. This approach leads to the consideration of several possible configurations for each number of rods removed so that a more reactive configuration is not inadvertently omitted. The differential reactivity effect of removing additional rods approaches zero at the point of peak reactivity, so no attempt is made to identify the optimum number of rods removed to the nearest single rod. The reactivities of several configurations would be statistically equivalent near this point. For the purposes of these analyses, the reactivity effect of this optimum condition has been sufficiently estimated.

4.2 LOSS OF CLADDING

The complete loss of all cladding material without subsequent collapse of fuel pellet material is a nonphysical assumption but is included in these analyses to provide an estimate of the reactivity worth of fuel cladding removal. The removal of the fuel cladding causes an increase in reactivity due to the removal of the absorptions in the cladding and the increased moderation within the assembly lattice. The moderation effect is the larger of the two components.

The models for loss of cladding remove the cladding material from the fuel rods. All Zircaloy-4 material is replaced with water, including the instrument and guide tubes.

4.3 LOSS OF ARRAY CONTROL

This scenario is based on failure of one or more of the assembly structural grids. This results in a loss of assembly array control. For these analyses, this is modeled as a uniform increase in the fuel rod pitch. The increased moderation within the assembly lattice causes an increase in reactivity. All fuel assemblies are assumed to undergo a uniform pitch expansion to completely fill the internal dimension of the storage cell.

The models for this scenario expand the fuel rod center-to-center spacing uniformly. The expansion is bounded by the internal dimension of the storage cell. For these analyses, the lattice is expanded until the outer boundary of the peripheral fuel rod unit cells is essentially in contact with the storage cell wall. For the BWR fuel, this expansion is performed both with and without the fuel channel present. The main difference is that the unchanneled assembly can expand farther without the constraint of the fuel channel. Also, for consistency with Ref. 7, the maximum pitch case is considered both with and without cladding present.

It is possible that a further increase could be realized if the fuel rod pitch were increased until the fuel rod was in contact with the cell wall instead of the fuel rod unit cell. For the purposes of these analyses, this potential increase was judged to be insignificant. Another potential factor that could exacerbate the reactivity increase would be a decrease in rod pitch in nonlimiting elevations adjacent to the limiting axial locations. This condition could result if the grids at the end of the assembly fail but grids remain intact farther from the end of the assembly.

4.4 POISON PANEL DAMAGE

The long-term performance of poison panels has not been good in spent fuel pools, as discussed in Ref. 21 and other sources. It is reasonable to assume that some degradation of the poison material or poison panels may occur in ES. The uncertainty regarding the environment that the panels may be exposed to over the duration of ES makes consideration of some sort of degradation or damage prudent. A range of scenarios is considered in these analyses to provide some estimates for the potential reactivity effects that could be associated with poison panel damage or degradation.

4.4.1 Limiting Elevation of Poison Damage

One aspect that can impact the reactivity effect of poison damage is the axial elevation of the poison defect. For these analyses the poison panel damage was assumed to be 5 cm tall and across the full width of the poison panel. Also, all poison panels in the cask were assumed to contain the same defect at the same elevation. This assumption will result in a conservative estimation of the reactivity increase due to poison panel damage.

In each of the cask models, a 5 cm gap is modeled in all poison panels at various elevations. For fresh fuel, the limiting elevation is most likely in the center of the assembly, so a few widely spaced intervals are used. For used fuel, the limiting elevation should shift to a position near the top end of the assembly. For these cases, a larger number of cases are investigated with finer spacing. The minimum spacing is slightly in excess of 5 cm, so a more detailed survey is likely to reveal a slight increase in the reactivity consequence of this poison degradation. For the purposes of these analyses, however, the resolution is sufficient to capture the vast majority of the reactivity effect.

4.4.2 Sensitivity to Extent of Damage

It is unlikely that the extent of any potential poison panel damage can be appropriately bounded without significant material testing. The sensitivity of the reactivity effect of poison damage to the size of the defect is therefore also estimated in these analyses. The magnitude of the sensitivity will provide some indication of the importance of poison material testing.

The sensitivity of the reactivity change to the extent of the poison panel damage is estimated by using 7.5 and 10 cm gaps. These larger gaps are modeled at the elevation determined to be limiting with the 5 cm gap cases discussed above in Section 4.4.1. As before, the larger gaps extend across the entire width and thickness of the poison panel. The defects also occur at the same elevation in all poisons panels. The sizes of the larger gaps are chosen arbitrarily.

4.4.3 Loss of a Single Panel

One of the most severe cases for poison panel degradation would be the loss of an entire panel. It is not expected that a single panel will be lost, but the scenario is included in these analyses for completeness.

The modeling of the loss of a single poison panel is straightforward. In all cases, a panel near the center of the cask is removed to maximize the effect of the missing panel. For the MPC-24 and MPC-68 casks, the stainless steel poison panel wrapper was also omitted.

4.5 ASSEMBLY AXIAL DISPLACEMENT

The poison panels in fuel storage and transportation casks are designed to overlap both ends of the active fuel, typically by as much as a few inches. In this context, it is important that the active fuel stay approximately in its intended position during and after ES. The cask designs use spacers to assure that the fuel assemblies are appropriately aligned. If the spacers or assembly end fittings fail, it is possible that the active fuel could shift axially into a region where no poison separates adjacent assemblies. The reactivity consequences of this condition are investigated in these analyses, both with and without the assumption that the assembly remains centered within the fuel storage cell. The maximum axial translation allowed is determined for the active fuel length neglecting the presence of all additional fuel assembly hardware above or below the pellet stack.

4.5.1 Pure Axial Displacement

Axial translation of a fuel assembly or multiple fuel assemblies would increase reactivity within the cask by relocating active fuel above or below the poison panels. This would allow for a significant increase in communication between adjacent assemblies, and a corresponding increase in reactivity.

The models of axial displacement translate all the fuel assemblies uniformly up or down into the lower and upper internal regions of the cask. The assemblies are moved in several relatively small intervals in an effort to map out the reactivity response as a function of displacement.

4.5.2 Eccentric Radial Position with Axial Displacement

Fuel assemblies that move out of position axially will likely also shift in the radial direction. The radial shift has the potential to exacerbate the reactivity increase caused by axial translation. The additional reactivity increase is caused by a further reduction in assembly spacing.

A series of different eccentric positions are considered for various casks in these analyses. Several of the variations included groupings of four assemblies misaligned toward the center of the 2×2 array of storage cells. A single group of four and multiple groups of four are considered in the GBC-32 and MPC-68 models. All three casks consider the case in which all assemblies are pushed toward the center of the cask. This should maximize the potential reactivity impact of axial and radial displacement.

4.6 GROSS ASSEMBLY FAILURE

The gross failure of the fuel assembly is a more realistic scenario than a failure of the cladding which leaves the fuel pellets in the fuel assembly lattice. Two scenarios for the physical form of the failed fuel are considered in these analyses: the first is a homogenous mixture of fuel and cladding materials and water, and the second is a dodecahedral array of fuel pellets suspended in water. The homogenous mixture is likely more representative of the condition of the assembly after any event significant enough to cause the simultaneous failure of all cladding material. This is especially true for irradiated fuel, in which the fuel pellets are already cracked and damaged from thermal stresses and radiation. The ordered array of pellets, while probably incredible, provides an upper bound of the reactivity of the fuel rubble since low enriched fuel is more reactive when lumped as compared to a homogeneous mixture. Each of the modeling techniques is described in more detail here.

4.6.1 Homogeneous Rubble

Irradiated fuel and cladding will suffer embrittlement from the high neutron fluence accumulated during core operations. This increases the probability that the cladding will lose ductility and will fail due to the impact caused by drop during transportation. The fuel pellets will, by the time the fuel has been discharged from the reactor, be significantly cracked from thermal stresses and similar radiation embrittlement. Assuming the fuel fails after the drop event, it is possible that the debris material will move through a range of volumes before settling to the bottom of the cask. For this reason, a series of total debris elevations is considered. This will also bound the range of possible final states of the cask following any mishandling during transportation.

The homogenous rubble scenario is modeled as occupying the internal volume of the fuel storage cell to varying elevations. The exact elevations used vary among the cask designs. All the cask designs are evaluated with the homogenous rubble replacing the fuel assembly in its original elevation. Other elevations include 40%, 60%, 80%, and 100% of the inside height of the cask. The volume occupied by water varies from about 21% to almost 74% of the homogenized mixture. A fully compressed case is also considered in which the fuel assembly debris has compacted to just fuel and cladding material, excluding all water. Some cask models also have state points for poison height and/or basket height. Most of these models contain rubble material above and/or below the poison panels, which are assumed to remain intact. In the full cask height scenarios, the fuel rubble is assumed to remain within the radial extent of the fuel storage cell, even above the storage basket. This is assumed mainly as a modeling convenience, and it likely reduces the reactivity of the configuration slightly. For the purposes of these analyses, however, the approximations are sufficient to provide a good estimate of the reactivity consequence of gross assembly failure leading to homogenous rubble within the cask.

4.6.2 Dodecahedral Array of Pellets

The case of gross assembly failure modeled as an ordered array of bare pellets is considered as a bound to the possible reactivity increase resulting from these scenarios. An ordered array of lumped low enriched fuel should lead to a greater reactivity increase for fuel assembly failure than the homogenous case described above because of resonance self-shielding of ^{238}U in low enriched fuel. The complete removal

of cladding is nonphysical, as discussed above in Section 4.2, but is again included to bound possible reactivity increases.

As with the homogeneous rubble case described above, a range of pellet array heights is considered. The entire internal area of the storage cell is assumed to be filled with the pellet array, also similar to the homogeneous rubble cases. The independent parameter for the dodecahedral array is the pitch, so a range of pitches is used in the models to achieve the different heights. Most of the cask models are evaluated with four different pitches/array heights. The minimum pitch in all cases maintains the height of the original fuel assembly, and the maximum pitch fills the inner area of the storage cell for the entire internal height of the cask. All dodecahedral array models are built in KENO-VI. A separate nominal model is developed in KENO-VI for each cask so that the reactivity increase of these pellet array models can be determined accurately.

Each of the cases is considered with two fuel pellet orientations. The pellets are aligned along the Z axis in one case and along the X axis in the other. An array of cylinders in a dodecahedral array cannot be modeled in a 1-D approximate geometry for cross section processing, so some approximate model is required. All the cases are run using the 1-D cross section processing model of a triangular array of spheres. This properly accounts for the dodecahedral array but does not properly capture the geometry of the fuel pellet. For the 1-D models, the fuel pellet is modeled as a sphere of the same volume of the fuel pellet. A small number of cases in which the pellets are aligned with the X axis also consider the 1-D model of cylindrical rods in a triangular array. The primary purpose of these calculations is to estimate the impact of the different cross section processing models.

4.7 PREFERENTIAL FLOODING (MPC-24 ONLY)

The MPC-24 is the only one of the three cask designs considered that integrates a flux trap into the design of the fuel storage basket. A flux trap is a region of typically water-filled space with poison panels on both sides of the trap, and is positioned between fuel storage cells. The worth of the poisons is greatly increased by allowing for additional moderation between the panels, thus allowing higher reactivity fuel to be stored safely. Fast neutrons escaping from one cell will be thermalized in the water between cells and are much more likely to be absorbed in the panel on the other side. For this design feature to be effective, the area within the flux trap must stay flooded in all cases in which the fuel storage cells are flooded. The primary design feature that precludes the drainage of only the flux traps is a semicircular opening in the bottom of the storage basket walls. These openings, called mouse holes, allow water to flow into all regions of the basket. Preferential flooding (i.e., flooding of the fuel storage cells but not the flux traps) is considered here.

The modeling of preferential flooding scenarios is straightforward. Two cases are considered: one in which only the flux traps are dry, and one in which the array inside the fuel storage cell but outside the fuel assembly is also dry. The latter case is essentially incredible but is included for completeness. No adjustments are needed to the cross section processing because the fuel assembly is always modeled as fully flooded.

5. RESULTS

This section reports the results of the calculations to determine the reactivity changes associated with each of the scenarios described above in Section 4. This section mostly presents data, with some analysis of the results. The conclusions that can be drawn from these results are presented separately in Section 6.

The results are presented in unique subsections for each cask. Any generic conclusions that apply to all cask and fuel types are presented explicitly in Section 6.4.

The uncertainty in all calculated reactivity differences presented in this section is approximately $0.00014 \Delta k_{\text{eff}}$, unless otherwise noted. The reported consequence is the difference in calculated k_{eff} values; the reported values are not divided by any k_{eff} values and therefore do not represent change in reactivity.

5.1 MPC-24

The reactivity change associated with each of the scenarios discussed in Section 4 is presented in this section for the MPC-24 cask. All scenarios assume a uniform loading of fresh 5 w/o Westinghouse 17×17 OFA fuel. The description of the fuel assembly modeling is provided in Section 3.2.1. A summary of the reactivity consequence of each scenario is provided in Table 4, with some additional details for each scenario provided in the subsequent subsections.

Table 4. Reactivity consequence summary for the MPC-24 cask

Scenario	Reactivity consequence (% Δk_{eff})
Single rod removal	0.15
Multiple rod removal	2.01
Cladding removal	5.24
Optimum pitch pellets	13.56
Homogenous mix	8.23
Axial displacement (maximum)	7.08
Axial displacement (20 cm)	0.03
Missing poison (5 cm segment)	0.35
Missing poison (10 cm segment)	1.07
Missing poison panel	0.44
Optimum rod pitch, clad	2.16
Optimum rod pitch, unclad	6.76
Optimum Flooding (dry flux traps)	16.61

5.1.1 Fuel Rod Collapse

Each of the 39 unique eighth-assembly symmetric rods is removed individually to determine its reactivity worth, as discussed in Section 4.1.1. Table 5 presents the rod locations whose best estimate worth is greater than $0.1\% \Delta k_{\text{eff}}$. Both the locations of these rods and the magnitude of the reactivity consequence of rod collapse are in good agreement with the previous work documented in Ref. 7. The columns in the assembly are designated with a letter, from A to Q, and the rows are designated with numbers, from 1 to 17. The maximum reactivity worth is associated with rod H8 and is $0.15\% \Delta k_{\text{eff}}$.

Multiple rods are removed in groups, as discussed in Section 4.1.2. For MPC-24, groups of 2, 4, 8, 12, 16, 24, 32, 40, 44, 48, and 52 rods are considered. The reactivity consequence is shown as a function of rods removed in Figure 7. The limiting lattice is shown in Figure 8. The maximum k_{eff} value occurs for 48 rods removed and corresponds to a reactivity increase of $2.01\% \Delta k_{\text{eff}}$.

**Table 5. Single rod removal results for
17×17 OFA in MPC-24**

Rod location	Reactivity consequence (% Δk_{eff})
H8	0.15
H5	0.13
H7	0.13
G5	0.12
I7	0.12
I8	0.12
I4	0.11
G7	0.11
G6	0.11

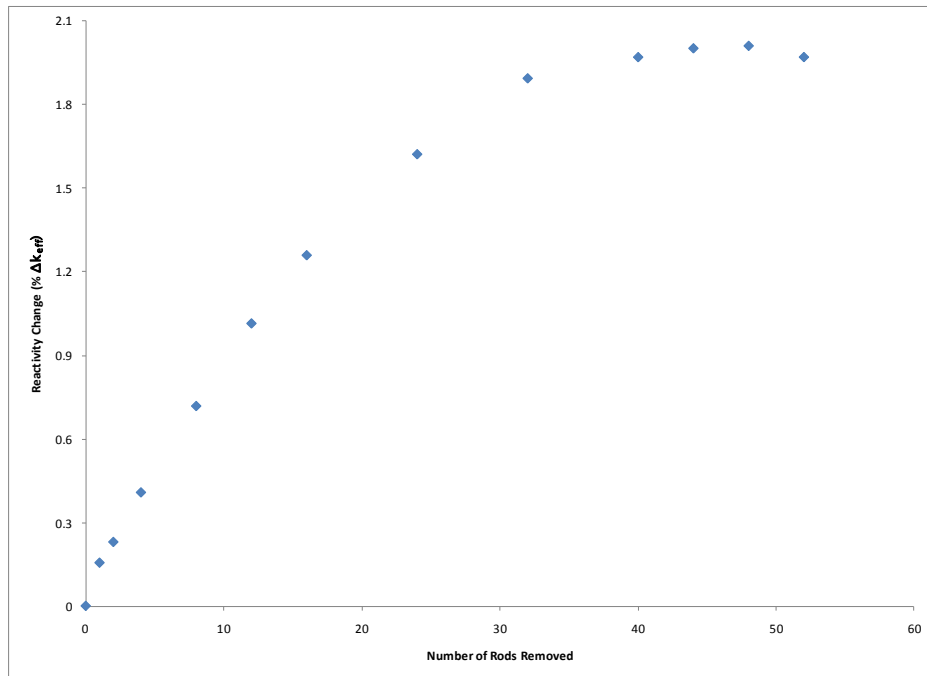


Figure 7. Reactivity change versus number of rods removed.

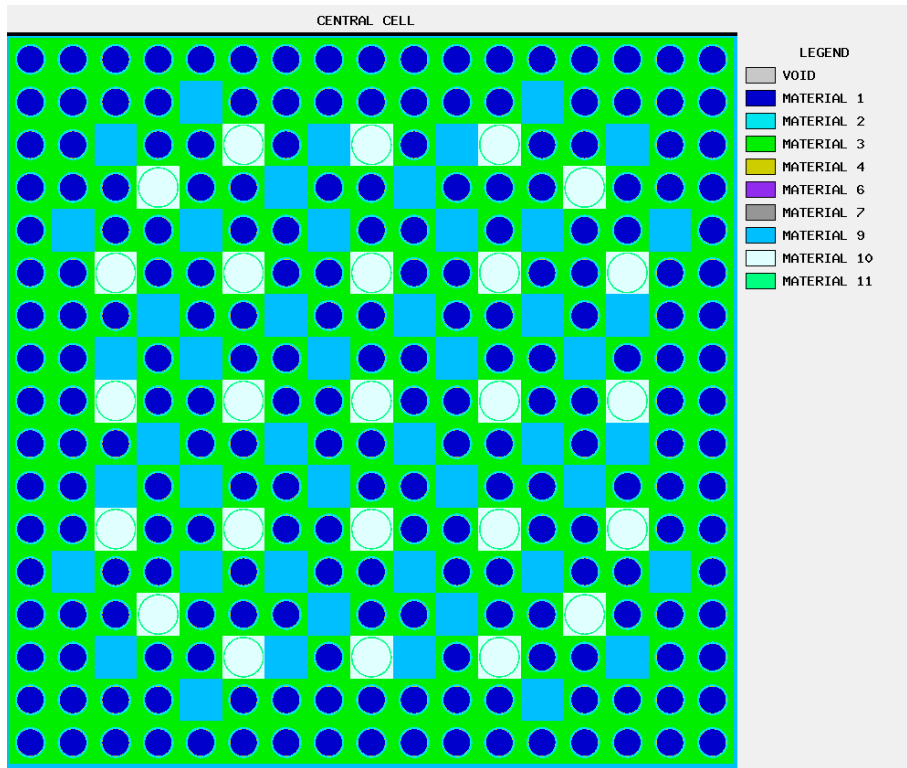


Figure 8. Limiting multiple rod removal lattice (48 rods removed).

5.1.2 Loss of Cladding

The loss of cladding scenario is modeled as discussed above in Section 4.2. As shown in Table 4, the reactivity increase associated with complete cladding removal is 5.24% Δk_{eff} . The results presented here are somewhat higher than those presented in Ref. 7. This may be due to a more rigorous cask model which includes the oversized fuel storage cells and the rotation of the standard storage cells relative to each other in the cask basket. These additional details may lead to a slightly more thermal spectrum and a correspondingly higher k_{eff} value for this scenario. Other changes in the analysis technique, including the use of an updated cross section library, may also influence the difference.

5.1.3 Loss of Array Control

The loss of array control is modeled as a uniform increase in fuel assembly pitch, as discussed above in Section 4.3. Two different fuel storage cell sizes exist in the MPC-24 basket, as discussed in Section 0. The four oversized storage cells allow for a larger uniform pitch than the 20 standard storage cells. The fuel assemblies in each type of cell are expanded to account for the larger possible pitch in the oversized storage cells. The maximum increase in k_{eff} , as shown in Table 4, is 2.16% Δk_{eff} with cladding intact and 6.76% with cladding removed. This agrees well with the results provided in Ref. 7.

5.1.4 Poison Panel Damage

The results of the calculations considering a 5 cm poison defect at varying elevations are presented in Table 6. The limiting elevation is, as expected for fresh fuel, at the centerline of the active fuel height. The reactivity increase for this location is 0.35% Δk_{eff} and increases to 1.07% Δk_{eff} if the defect size is increased to 10 cm. As discussed in Sections 4.4.1 and 0, these defects are assumed to be present at the

same elevation in all poison panels within the cask. The consequence of the removal of a poison panel near the center of the cask is 0.44% Δk_{eff} . Poison damage and degradation was not considered in Ref. 7, so no comparison is possible.

Table 6. Reactivity insertion of a 5 cm poison defect at various elevations

Defect elevation midpoint (cm above bottom of active fuel)	Reactivity consequence (% Δk_{eff})
2.50	0.03
91.44	0.28
182.88	0.35
274.32	0.26
363.26	0.03

5.1.5 Assembly Axial Displacement

The assembly misalignment scenario is calculated over a range of displacements, as shown in Figure 9. The consequence of the maximum misalignment is quite large, at over 7% Δk_{eff} . The results provided in Table 4 therefore also present a more limited misalignment. This 20 cm misalignment accounts for some degradation of assembly end fittings or the spacers used inside the cask to ensure proper assembly alignment. For the fresh fuel in the MPC-24 cask, this limited misalignment case has significantly less worth.

Eccentric positioning of the fresh misaligned assemblies increases the reactivity consequence of the scenario. The reactivity increase in the limited misalignment case is approximately 0.1% Δk_{eff} , but the consequence in the maximum misalignment case is 1.17% Δk_{eff} . The total possible reactivity insertion due to complete loss of assembly alignment is over 8% Δk_{eff} .

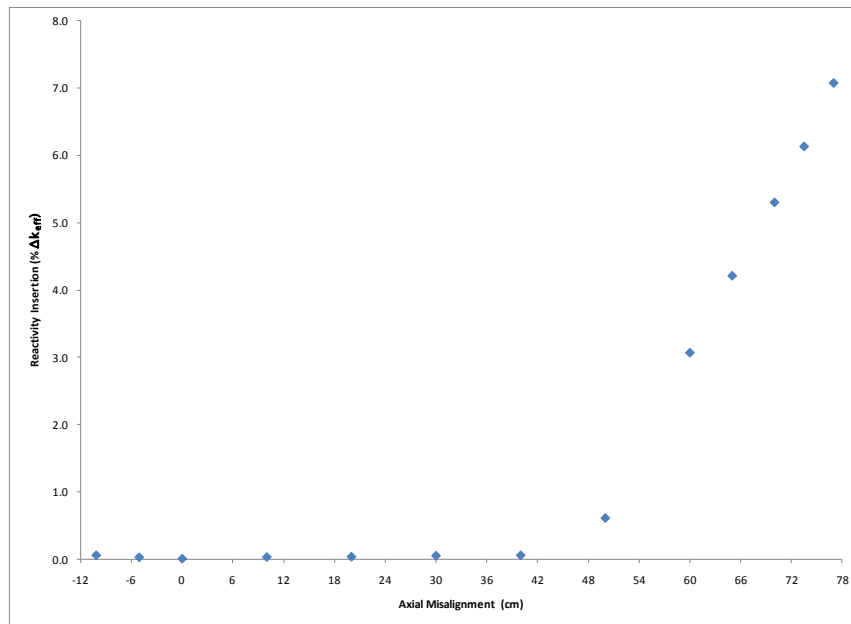


Figure 9. Reactivity consequence versus axial assembly misalignment in MPC-24.

5.1.6 Gross Assembly Failure

The two gross assembly failure scenarios described in Section 4.6 are investigated in the MPC-24 cask. As expected, this scenario has the highest reactivity increase: the pellet array case has a larger k_{eff} increase than the homogeneous rubble case. As shown in Table 4, the reactivity increase in the homogeneous rubble case is over 8% Δk_{eff} , and the pellet array case increases reactivity by over 13.5% Δk_{eff} .

The results for the pellet array case are significantly higher than those reported previously in Ref. 7. This is primarily because the array is also allowed to extend beyond the poison panel elevations. The homogeneous rubble case was not included in Ref. 7.

5.1.7 Preferential Flooding

The preferential flooding scenario that leaves the flux traps dry in the basket is considered only for the MPC-24 cask, as mentioned in Section 4.7. The results, as shown in Table 4, indicate a potential reactivity insertion of more than 16.5% Δk_{eff} in this case. The importance of the flux traps, and the elimination of the potential for a preferential flooding scenario, is clearly demonstrated.

5.2 GBC-32

The reactivity change associated with each of the reconfiguration scenarios discussed in Section 4 is presented in this section for the GBC-32 cask. The scenarios assume a range of loadings of Westinghouse 17×17 OFA fuel. The description of the fuel assembly modeling is provided in Section 3.2.1. The enrichments, burnups, and cooling times used are presented in Table 7. The rationale used to select these points is provided in Section 3.1.2. A summary of the reactivity consequence of each scenario is provided in Table 8, with some additional details for each scenario and the results for all seven state points provided in the subsequent subsections.

Table 7. Enrichment, burnup, and cooling time for state points considered in GBC-32

Enrichment (w/o ^{235}U)	Burnups (MWd/MTU)	Cooling times (years)
1.92	0	0
5.0	44,250	5
		80
		300
	70,000	5
		80
		300

Table 8. Reactivity consequence summary for the GBC-32 cask

Scenario	Reactivity consequence (% Δk_{eff})	Limiting condition	
		Burnup (MWd/MTU)	Cooling time (years)
Single rod removal	0.10	44250	300
Multiple rod removal	1.86	44250	80
Cladding removal	3.52	44250	80
Optimum pitch pellets	22.21	44250	80
Homogenous mix	15.34	44250	300
Axial displacement (maximum)	17.38	44250	300
Axial displacement (20 cm)	12.49	70000	300
Missing poison (5 cm segment)	1.24	70000	300
Missing poison (10 cm segment)	2.63	70000	300
Missing poison panel	1.08	0	0
Optimum rod pitch, clad	1.69	44250	5
Optimum rod pitch, unclad	4.89	44250	5

5.2.1 Fuel Rod Collapse

Each of the 39 eighth-assembly symmetric rods is removed individually to determine its reactivity worth, as discussed in Section 4.1.1. Table 9 presents the rod locations and worth of the limiting rod location for each of the seven cases. Both the locations of these rods and the magnitude of the reactivity consequence of rod collapse are in good agreement with the previous work documented in Ref. 7. The columns in the assembly are designated with a letter, from A to Q, and the rows are designated with numbers, from 1 to 17. The maximum reactivity worth is associated with rod G7 at 44,250 MWd/MTU burnup and 300 years of cooling time. The limiting location, G7, is similar to the limiting location for the MPC-24 cask. G7 and H8 are diagonally adjacent locations. Both are in the central region of the assembly, and these central locations are limiting because they are farthest from the periphery of the assembly. The removal of peripheral rods lowers reactivity because it increases leakage, while the reactivity is increased by the removal of interior rods because of an increase in moderation within the lattice. The reactivity worth is 0.1% Δk_{eff} . It should be noted that several rods across many of the state points have a reactivity worth that is statistically equivalent to this particular limiting case. The worth is very small relative to the reactivity consequence of other scenarios, so further examination is not necessary.

Multiple rods are removed in groups, as discussed in Section 4.1.2. For GBC-32, groups of 2, 4, 8, 16, 24, 28, 32, 36, 40, 44, and 48 rods are considered. The reactivity consequence is shown for each of the cases in Table 10. Figure 10 shows the reactivity insertion as a function of rods removed for the limiting case at 44,250 MWd/MTU burnup and 300 years of cooling time. The limiting lattice is shown in Figure 11. The maximum k_{eff} value occurs for 44 rods removed and corresponds to a reactivity increase of 1.87% Δk_{eff} . The reactivity increase for multiple rod removal in the GBC-32 cask is somewhat higher here than in Ref. 7. This is most likely due to the use of distributed burnup profile models in this work as compared to a uniform burnup profile in the previous analysis.

Multiple rod removal in the fresh fuel 1.92 w/o case caused the cask reactivity to decrease, so a very small penalty is identified. Single rod removal bounds all multiple rod removal scenarios considered in that case. Note that for fresh fuel the limiting location is H8, which is the same location as the fresh fuel in the MPC-24 cask.

Table 9. Single rod removal results for 17×17 OFA in GBC-32

Burnup (MWd/MTU)	Cooling time (years)	Location	Reactivity consequence (% Δk_{eff})
0	0	H8	0.04
44250	5	H5	0.10
44250	80	H7	0.09
44250	300	G7	0.10
70000	5	H5	0.09
70000	80	G7	0.10
70000	300	G5	0.10

Table 10. Multiple rod removal results for 17×17 OFA in GBC-32

Burnup (MWd/MTU)	Cooling time (years)	Reactivity consequence (% Δk_{eff})
0	0	0.03
44250	5	1.86
44250	80	1.86
44250	300	1.87
70000	5	1.69
70000	80	1.62
70000	300	1.62

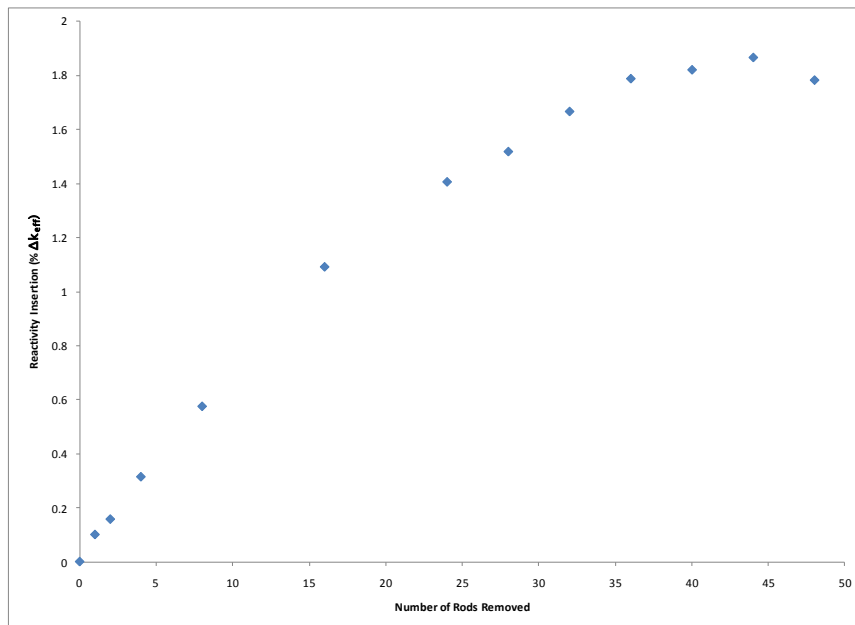


Figure 10. Reactivity change versus number of rods removed.

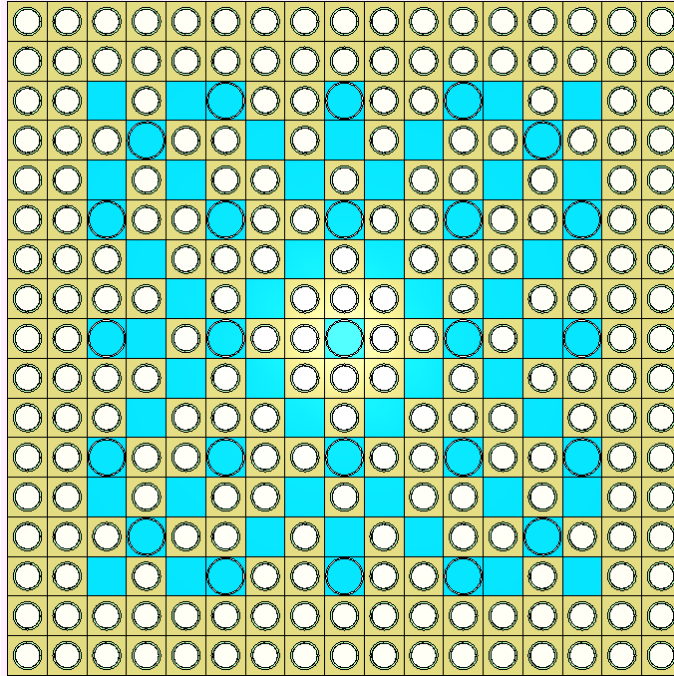


Figure 11. Limiting multiple rod removal lattice (44 rods removed).

5.2.2 Loss of Cladding

The loss of cladding scenario is modeled as discussed above in Section 4.2. As shown in Table 8, the limiting reactivity increase associated with complete cladding removal is 3.52% Δk_{eff} and occurs for the 44,250 MWd/MTU burnup case with 80 years of cooling time. The results for all seven cases are summarized in Table 11. The results are in good agreement with those presented in Ref. 7.

Table 11. Reactivity consequence for cladding removal in GBC-32

Burnup (MWd/MTU)	Cooling time (years)	Reactivity consequence (% Δk_{eff})
0	0	2.81
44250	5	3.49
44250	80	3.52
44250	300	3.19
70000	5	3.34
70000	80	3.28
70000	300	3.33

5.2.3 Loss of Array Control

The loss of array control is modeled as a uniform increase in fuel assembly pitch, as discussed above in Section 4.3. The fuel assemblies in each cell are expanded uniformly to fill the inner dimensions of the storage cells. The maximum increase in k_{eff} , as shown in Table 8, is 1.69% Δk_{eff} with cladding intact and 4.89% with cladding removed. The limiting condition for both cases is the minimum five year cooling

time for fuel with 44,250 MWd/MTU burnup. The results for all seven cases, both with and without cladding, are shown in Table 12. No results for this scenario are presented in Ref. 7.

Table 12. Results for loss of array control in GBC-32

Burnup (MWd/MTU)	Cooling time (years)	Reactivity consequence (% Δk_{eff})
Cladding intact		
0	0	0.78
44250	5	1.69
44250	80	1.67
44250	300	1.66
70000	5	1.53
70000	80	1.44
70000	300	1.42
Cladding removed		
0	0	3.30
44250	5	4.89
44250	80	4.86
44250	300	4.87
70000	5	4.58
70000	80	4.43
70000	300	4.46

5.2.4 Poison Panel Damage

The limiting results of the calculations considering a 5 cm poison defect at varying elevations for all seven cases are presented in Table 13. The limiting condition is for fuel with 70,000 MWd/MTU burnup and 300 years of cooling time. The limiting elevation is, as expected for depleted fuel, near the top of the active fuel height. The results for the full range of elevations considered in the limiting fuel condition are presented in Table 14. The limiting elevation for the fresh 1.92 w/o fuel is located as the centerline, as expected for fresh fuel and consistent with the results for MPC-24 presented in Section 5.1.4. The limiting reactivity increase for this scenario is 1.24% Δk_{eff} and increases to 2.63% Δk_{eff} if the defect size is increased to 10 cm. As discussed in Sections 4.4.1 and 0, these defects are assumed to be present at the same elevation in all poison panels within the cask. The consequence of the removal of a poison panel near the center of the cask is 1.08% Δk_{eff} and occurs for the fresh 1.92 w/o fuel. Table 15 provides the reactivity consequence for a single missing panel for all seven cases considered in the GBC-32 cask. Poison damage and degradation was not considered in Ref. 7, so no comparison is possible.

Table 13. Maximum reactivity insertion of a 5 cm poison defect in GBC-32

Burnup (MWd/MTU)	Cooling Time (years)	Defect elevation (cm)	Reactivity consequence (% Δk_{eff})
0	0	182.88	0.29
44250	5	348.86	1.05
44250	80	348.86	1.22
44250	300	348.86	1.21
70000	5	348.86	1.17
70000	80	348.86	1.24
70000	300	348.86	1.24

Table 14. Reactivity insertion of a 5 cm poison defect at various elevations in GBC-32 (70,000 MWd/MTU BU and 300 year cooling time)

Defect elevation (cm)	Reactivity consequence (% Δk_{eff})
321.77	0.12
328.54	0.30
335.31	0.53
342.09	0.85
348.86	1.24
355.64	1.17

Table 15. Reactivity consequence of a single missing panel in GBC-32

Burnup (MWd/MTU)	Cooling time (years)	Reactivity consequence (% Δk_{eff})
0	0	1.08
44250	5	0.90
44250	80	0.89
44250	300	0.89
70000	5	0.83
70000	80	0.80
70000	300	0.79

5.2.5 Assembly Axial Displacement

The assembly misalignment scenario is calculated over a range of displacements. The consequence of the maximum misalignment for all seven cases is shown in Table 16 and is over 17% Δk_{eff} for the limiting condition. The results provided in Table 8 therefore also present a more limited misalignment. This 20 cm misalignment accounts for some degradation of assembly end fittings or the spacers used inside the cask to ensure proper assembly alignment. This limited misalignment case has significantly less worth, but the reactivity insertion is still nearly 12.5% Δk_{eff} , as shown in Table 17. The limiting condition for the maximum misalignment is for fuel with 44,250 MWd/MTU burnup and 300 years cooling time, but it changes to a burnup of 70,000 MWd/MTU for the limited misalignment case. Misalignment toward the

bottom of the cask has significantly less reactivity impact because the fuel at the bottom end of the assembly has lower reactivity. The variation of the reactivity consequence as a function of axial position is shown in Figure 12 for fuel with 44,250 MWd/MTU burnup and 300 years of cooling time.

Eccentric positioning of the misaligned assemblies does increase the reactivity consequence of the reconfiguration scenario. The largest reactivity increase in the maximum misalignment case is approximately 0.5% Δk_{eff} , but this occurs for fresh fuel. The effect of eccentricity for depleted fuel conditions is slightly less. The total possible reactivity insertion due to complete loss of assembly alignment is over 17.8% Δk_{eff} .

Table 16. Reactivity consequence for assembly axial displacement in GBC-32

Burnup (MWd/MTU)	Cooling time (years)	Reactivity consequence (% Δk_{eff})
0	0	10.38
44250	5	16.70
44250	80	17.37
44250	300	17.38
70000	5	16.88
70000	80	16.93
70000	300	17.05

Table 17. Reactivity consequence for limited assembly axial displacement in GBC-32

Burnup (MWd/MTU)	Cooling time (years)	Reactivity consequence (% Δk_{eff})
0	0	3.85
44250	5	10.82
44250	80	11.82
44250	300	11.77
70000	5	11.74
70000	80	12.46
70000	300	12.49

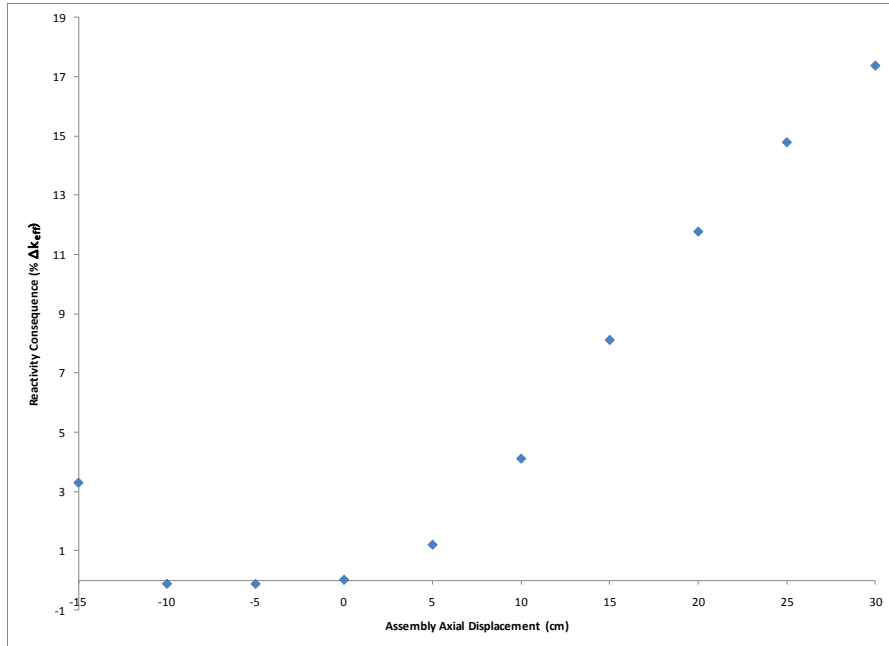


Figure 12. Reactivity consequence versus assembly axial displacement (44,250 MWd/MTU BU and 300 year cooling time).

5.2.6 Gross Fuel Assembly Failure

The two gross assembly failure scenarios described in Section 4.6 are investigated in the GBC-32 cask. As expected, this scenario as modeled has the highest reactivity increase, and the pellet array case is more limiting than the homogeneous rubble case. As shown in Table 8, the reactivity increase in the homogeneous rubble case is over 15% Δk_{eff} , and the pellet array case increases reactivity by over 22% Δk_{eff} . The limiting homogeneous rubble case is for the 44,250 MWd/MTU burnup case with 300 years cooling time, while the limiting pellet array case is with 80 years of cooling time. The results for both scenarios for all seven fuel conditions are presented in Table 18 and illustrate that the 80 and 300 year cooling times are essentially equivalent.

The results for the pellet array case are significantly higher than those reported previously in Ref. 7. There are two main differences between that analysis and this one, both of which contribute to a sizeable reactivity increase in the work presented here. The pellet array case modeled here includes the distributed burnup profile in the pellet array. The array is also allowed to extend beyond the poison panel elevations. This latter change is the larger of the two effects, but the former change is also important. The homogeneous rubble case was not included in Ref. 7.

Table 18. Reactivity consequence of gross fuel assembly failure in GBC-32

Burnup (MWd/MTU)	Cooling time (years)	Reactivity consequence (% Δk_{eff})
Limiting pellet array		
0	0	11.09
44250	5	21.37
44250	80	22.21
44250	300	22.21
70000	5	21.43
70000	80	21.63
70000	300	21.77
Homogeneous rubble		
0	0	6.66
44250	5	14.30
44250	80	15.29
44250	300	15.34
70000	5	14.20
70000	80	14.77
70000	300	14.90

5.3 MPC-68

The reactivity change associated with each of the reconfiguration scenarios discussed in Section 4 is presented here for the MPC-68 cask. The scenarios assume a range of loadings of GE 10×10 fuel. The description of the fuel assembly modeling is provided in Section 3.2.2. All fuel is modeled with a uniform initial enrichment of 5 w/o. The burnups and cooling times used are presented in Table 19. The basis for selecting these points is provided in Section 3.2.2. All scenarios, with the exception of the uniform array of pellets in the gross fuel assembly failure scenario, also considered the fuel both with and without the channel present. A summary of the reactivity consequence of each scenario is provided in Table 20. Some additional details for each scenario and the results for all seven state points are provided in the subsequent subsections.

Comparing the results of these analyses to those presented in Ref. 7 is more difficult for the MPC-68 cask than for the MPC-24 of GBC-32 casks. The difficulty is primarily a result of the analyses in Ref. 7 using an 8×8 fuel assembly.

Table 19. Burnup and cooling times considered in MPC-68

Burnups (MWd/MTU)	Cooling Times (years)
0	0
	5
35,000	80
	300
	5
70,000	80
	300

Table 20. Reactivity consequence summary for the MPC-68 cask

Scenario	Reactivity consequence (% Δk_{eff})	Limiting condition		
		Burnup (MWd/MTU)	Cooling time (years)	Channel present
Single rod removal	0.29	0	0	Yes
Multiple rod removal	2.42	35	300	Yes
Cladding removal	4.98	0	0	Yes
Optimum pitch pellets	35.63	70	300	No
Homogenous mix	30.40	70	300	No
Axial displacement (maximum)	20.76	70	300	Yes
Axial displacement (20 cm)	8.52	70	80	Yes
Missing poison (5 cm segment)	2.90	70	80	Yes
Missing poison (10 cm segment)	6.36	70	300	Yes
Missing poison panel	0.71	0	0	Yes
Optimum rod pitch, clad	12.07	0	0	No
Optimum rod pitch, unclad	14.70	0	0	No

5.3.1 Fuel Rod Collapse

Each of the 51 unique half-assembly symmetric rods is removed individually to determine its reactivity worth, as discussed in Section 4.1.1. Table 21 presents the rod locations and worth of the limiting rod location for each of the seven cases. In all seven cases, the reactivity increase for the channeled fuel assembly is greater than the reactivity increase for the unchanneled assembly. This is explained below, as it is also true for the multiple rod collapse scenarios.

The magnitude of the reactivity consequence of rod collapse is somewhat less for these analyses than for the previous work documented in Ref. 7. The primary cause of the reduction is the difference in the size of the fuel rods. The fuel rods in the 10×10 fuel assembly have smaller diameters, so the increase in moderation is smaller for a single rod removal.

The columns in the assembly are designated with a letter, from A to J, and the rows are designated with numbers, from 1 to 10. The maximum reactivity worth is associated with rod H7 with fresh 5 w/o fuel. The reactivity worth is 0.29% Δk_{eff} . It should be noted that some rods across a few of the state points have a reactivity worth that is statistically equivalent to this particular limiting case. The worth is very small relative to the reactivity consequence of other scenarios, so further examination is not necessary.

Multiple rods are removed in groups, as discussed in Section 4.1.2. For MPC-68, groups of 2, 3, 4, 6, 8, 10, 12, 14, 16, 18, and 20 rods are considered. The reactivity consequence is shown for each of the seven cases in Table 22. Figure 13 shows the reactivity insertion as a function of rods removed for the limiting case at 35,000 MWd/MTU burnup and 300 years of cooling time with the fuel assembly channel. The limiting lattice is shown in Figure 14. The maximum k_{eff} value occurs for 18 rods removed and corresponds to a reactivity increase of 2.42% Δk_{eff} .

The limiting lattice is determined with the fuel channel intact and then re-run with the fuel channel removed. In each case, the reactivity increase is higher with the channel intact. This is likely caused by the slightly harder initial spectrum when the channel is present. The increase in moderation caused by the removal of the fuel rods has a greater impact on the harder initial spectrum.

The reactivity increase for multiple rod removal in the MPC-68 cask is about twice that reported in Ref. 7. This is most likely due to the difference in the fuel assembly modeled in the analysis. The result for fresh fuel shown in Table 22 demonstrates that the effect of depleted fuel instead of fresh fuel is small.

Table 21. Single rod removal results for GE 10×10 fuel in MPC-68

Burnup (MWd/MTU)	Cooling time (years)	Reactivity consequence (% Δk_{eff})
0	0	0.29
35,000	5	0.26
35,000	80	0.27
35,000	300	0.28
70,000	5	0.26
70,000	80	0.25
70,000	300	0.26

Table 22. Multiple rod removal results for GE 10×10 fuel in MPC-68

Burnup (MWd/MTU)	Cooling time (years)	Reactivity consequence (% Δk_{eff})
0	0	2.24
35,000	5	2.40
35,000	80	2.40
35,000	300	2.42
70,000	5	2.30
70,000	80	2.31
70,000	300	2.32

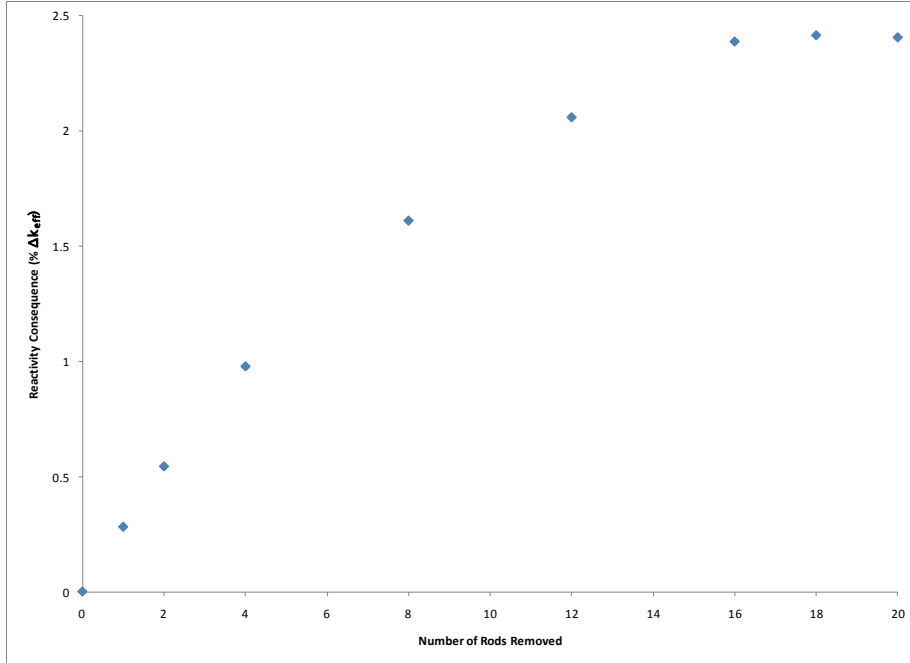


Figure 13. Reactivity change versus number of rods removed.

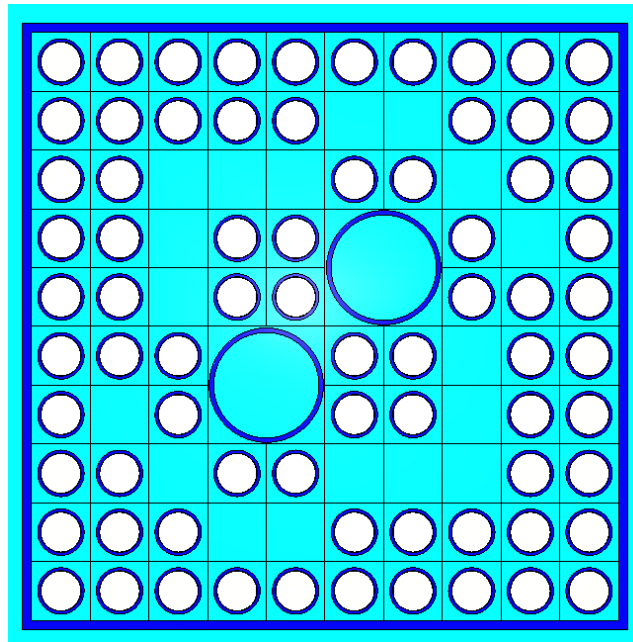


Figure 14. Limiting multiple rod removal lattice (18 rods removed).

5.3.2 LOSS OF CLADDING

The loss of cladding scenario is modeled as discussed above in Section 4.2. As shown in Table 20, the limiting reactivity increase associated with complete cladding removal is 4.98% Δk_{eff} and occurs with

fresh fuel. The results for all seven cases, both with and without the fuel channel, are summarized in Table 23. The results are in good agreement with those presented in Ref. 7.

Table 23. Reactivity consequence for cladding removal in MPC-68

Burnup (MWd/MTU)	Cooling time (years)	Reactivity consequence (% Δk_{eff})
Channel intact		
0	0	4.98
35,000	5	4.82
35,000	80	4.82
35,000	300	4.84
70,000	5	4.69
70,000	80	4.67
70,000	300	4.70
Channel removed		
0	0	4.71
35,000	5	4.59
35,000	80	4.62
35,000	300	4.59
70,000	5	4.48
70,000	80	4.47
70,000	300	4.47

5.3.3 Loss of Array Control

The loss of array control is modeled as a uniform increase in fuel assembly pitch, as discussed above in Section 4.3. The fuel assemblies in each cell are expanded uniformly to fill the inner dimensions of the storage cells. For the BWR fuel, the presence of the fuel channel acts to restrain the uniform pitch increase by the thickness of the channel wall on both sides. This causes lower pitch and reactivity increases compared to the unchanneled fuel cases. The maximum increase in k_{eff} , as shown in Table 20, is more than 12% Δk_{eff} with cladding intact and 14.7% with cladding removed. The limiting condition for both cases is with fresh fuel. The results for all seven cases with cladding, with and without the fuel channel, are shown in Table 24. The results for all seven cases without cladding, with and without the fuel channel, are shown in Table 25.

The results presented here show a larger increase in reactivity than that reported in Ref. 7. This is probably a result of the different fuel assembly lattice. Figure 21 in Ref. 7 indicates that the reactivity consequence of uniform pitch expansion increases with the array size. The effects of the different fuel rod and water tube diameters in the 10×10 fuel are not accounted for in Ref. 7, however, so it is possible that these factors also influence the difference between the two analyses.

Table 24. Results for loss of array control with cladding intact in MPC-68

Burnup (MWd/MTU)	Cooling time (years)	Reactivity consequence (% Δk_{eff})
Channel intact		
0	0	11.00
35,000	5	9.55
35,000	80	9.46
35,000	300	9.49
70,000	5	8.68
70,000	80	8.51
70,000	300	8.52
Channel removed		
0	0	12.07
35,000	5	10.56
35,000	80	10.45
35,000	300	10.48
70,000	5	9.64
70,000	80	9.40
70,000	300	9.43

Table 25. Results for loss of array control without cladding in MPC-68

Burnup (MWd/MTU)	Cooling time (years)	Reactivity consequence (% Δk_{eff})
Channel intact		
0	0	14.05
35,000	5	12.74
35,000	80	12.65
35,000	300	12.69
70,000	5	11.87
70,000	80	11.74
70,000	300	12.62
Channel removed		
0	0	14.70
35,000	5	13.30
35,000	80	13.26
35,000	300	13.26
70,000	5	12.42
70,000	80	12.26
70,000	300	12.30

5.3.4 Poison Panel Damage

The limiting results of the calculations considering a 5 cm poison defect at varying elevations for all seven cases, both with and without the fuel channel, are presented in Table 26. The limiting condition is for fuel with 70,000 MWd/MTU burnup and 80 years of cooling time, with the fuel channel intact. The limiting elevation is, as expected for depleted fuel, near the top of the active fuel height. The results for the full range of elevations considered in the limiting fuel condition are presented in Table 27 for cases with the fuel channel intact. The limiting elevation for the fresh 5 w/o fuel is located at the centerline, as expected for fresh fuel and consistent with the results for MPC-24 and GBC-32 presented in Sections 5.1.4 and 5.2.4. The limiting reactivity increase for this scenario is 2.90% Δk_{eff} and increases to 6.36% Δk_{eff} if the defect size is increased to 10 cm. The limiting condition for the 10 cm gap also changes to the 300 year cooling time with 70,000 MWd/MTU burnup fuel. As discussed in Sections 4.4.1 and 0, these defects are assumed to be present at the same elevation in all poison panels within the cask. The consequence of the removal of a poison panel near the center of the cask is 0.71% Δk_{eff} and occurs for the fresh fuel. Table 28 provides the reactivity consequence for a single missing panel for all seven cases considered in the MPC-68 cask, both with and without the presence of the fuel channel. Poison damage and degradation was not considered in Ref. 7, so no comparison is possible.

Table 26. Maximum reactivity insertion of a 5 cm poison defect in MPC-68

Burnup (MWd/MTU)	Cooling time (years)	Defect elevation (cm)	Reactivity consequence (% Δk_{eff})
Channel intact			
0	0	190.50	0.83
35,000	5	365.13	2.49
35,000	80	365.13	2.58
35,000	300	365.13	2.58
70,000	5	370.42	2.82
70,000	80	370.42	2.90
70,000	300	370.42	2.89
Channel removed			
0	0	190.50	0.77
35,000	5	365.13	2.41
35,000	80	365.13	2.53
35,000	300	365.13	2.51
70,000	5	370.42	2.75
70,000	80	370.42	2.81
70,000	300	370.42	2.82

Table 27. Reactivity insertion of a 5 cm poison defect at various elevations in MPC-68 (70,000 MWd/MTU BU and 80 year cooling time)

Defect elevation (cm)	Reactivity consequence (% Δk_{eff})
0.00	-0.01
95.25	-0.01
190.50	0.01
285.75	-0.01
317.50	0.00
333.38	0.02
349.25	0.45
354.54	0.91
359.83	1.78
365.13	2.47
370.42	2.90
375.71	2.87
381.00	1.23

Table 28. Reactivity consequence of a single missing panel in MPC-68

Burnup (MWd/MTU)	Cooling time (year)	Reactivity consequence (% Δk_{eff})
Channel intact		
0	0	0.71
35,000	5	0.58
35,000	80	0.58
35,000	300	0.60
70,000	5	0.54
70,000	80	0.54
70,000	300	0.57
Channel removed		
0	0	0.63
35,000	5	0.59
35,000	80	0.58
35,000	300	0.56
70,000	5	0.55
70,000	80	0.50
70,000	300	0.51

5.3.5 Assembly axial displacement

The assembly misalignment scenario is calculated over a range of displacements. The consequence of the maximum misalignment for the six cases involving depleted fuel, both with and without the assembly channel, is shown in Table 29 and is over 20% Δk_{eff} for the limiting condition. The results provided in Table 20 therefore also present a more limited misalignment. This 20 cm misalignment accounts for some degradation of assembly end fittings or the spacers used inside the cask to ensure proper assembly alignment. This limited misalignment case has significantly less worth, but the reactivity insertion is still over 8.5% Δk_{eff} , as shown in Table 30. The limiting condition for the maximum misalignment is for fuel

with 70,000 MWd/MTU burnup and 300 years cooling time, but it changes to a burnup of 80 years of cooling time for the limited misalignment case. Misalignment toward the bottom of the cask has significantly less reactivity impact because the fuel at the bottom end of the assembly has lower reactivity. The variation of the reactivity consequence as a function of axial position is shown in Figure 15 for fuel with 70,000 MWd/MTU burnup and 300 years of cooling time.

Eccentric positioning of the misaligned assemblies increases the reactivity consequence of the reconfiguration scenario. The largest reactivity increase in the maximum misalignment case is approximately 2% Δk_{eff} , but this occurs for fuel with 35,000 MWd/MTU burnup and 5 years of cooling time. The effect of eccentricity for fuel with 70,000 MWd/MTU burnup is slightly less. The total reactivity insertion due to complete loss of assembly alignment is over 22.5% Δk_{eff} .

Table 29. Reactivity consequence for assembly axial displacement in MPC-68

Burnup (MWd/MTU)	Cooling time (years)	Reactivity consequence (% Δk_{eff})
Channel intact		
35,000	5	19.40
35,000	80	19.84
35,000	300	19.82
70,000	5	20.47
70,000	80	20.73
70,000	300	20.76
Channel removed		
35,000	5	18.65
35,000	80	19.10
35,000	300	19.06
70,000	5	19.71
70,000	80	19.96
70,000	300	20.00

Table 30. Reactivity consequence for limited assembly axial displacement in MPC-68

Burnup (MWd/MTU)	Cooling time (years)	Reactivity consequence (% Δk_{eff})
Channel intact		
35,000	5	6.29
35,000	80	6.70
35,000	300	6.66
70,000	5	8.03
70,000	80	8.52
70,000	300	8.49
Channel removed		
35,000	5	6.07
35,000	80	6.49
35,000	300	6.42
70,000	5	7.78
70,000	80	8.24
70,000	300	8.20

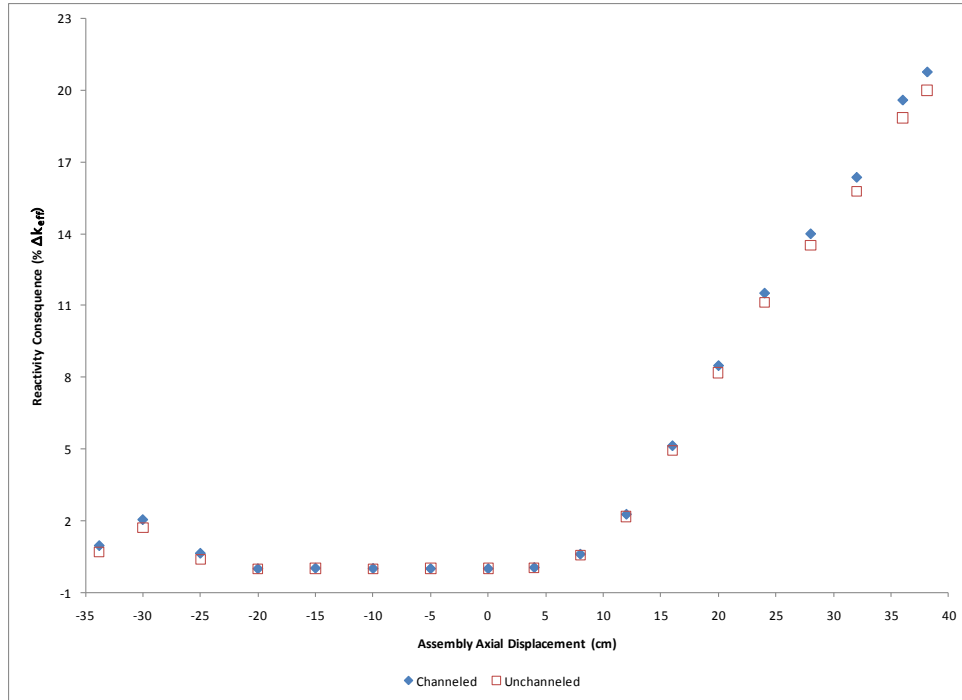


Figure 15. Reactivity consequence versus assembly axial displacement.

5.3.6 Gross Fuel Assembly Failure

The two gross assembly failure scenarios described in Section 4.6 are investigated in the MPC-68 cask. As expected, this scenario has the highest reactivity increase, with the pellet array case being more limiting than the homogeneous rubble case. As shown in Table 20, the reactivity increase in the homogeneous rubble case is over 30% Δk_{eff} , and the pellet array case increases reactivity by over 35% Δk_{eff} . The limiting case for both scenarios is with fuel at 70,000 MWd/MTU burnup and 300 years cooling time. The results for the homogeneous scenario for all seven fuel conditions with and with the fuel channel are presented in Table 31. The results for the pellet array case for all seven fuel conditions are shown in Table 32. The pellet array case was only considered without the fuel assembly channel.

The results for the pellet array case are significantly higher than those reported previously in Ref. 7. There are two differences between that analysis and this one, both of which contribute to the increased reactivity consequence in the work presented here. The pellet array case modeled here includes the distributed burnup profile in the pellet array. The array is also allowed to extend beyond the poison panel elevations. This latter change is the larger of the two effects, but the former change is also important. The homogeneous rubble case was not included in Ref. 7.

Table 31. Reactivity consequence of homogeneous rubble scenario of gross fuel assembly failure in MPC-68

Burnup (MWd/MTU)	Cooling time (years)	Reactivity consequence (% Δk_{eff})
Channel intact		
0	0	21.68
35,000	5	28.58
35,000	80	29.12
35,000	300	29.13
70,000	5	29.31
70,000	80	29.74
70,000	300	29.81
Channel removed		
0	0	22.90
35,000	5	29.36
35,000	80	29.87
35,000	300	29.83
70,000	5	29.93
70,000	80	30.33
70,000	300	30.40

Table 32. Reactivity consequence of pellet array scenario of gross fuel assembly failure in MPC-68

Burnup (MWd/MTU)	Cooling time (years)	Reactivity consequence (% Δk_{eff})
Channel removed		
0	0	28.12
35,000	5	34.40
35,000	80	34.88
35,000	300	34.87
70,000	5	35.22
70,000	80	35.57
70,000	300	35.63

6. SUMMARY AND CONCLUSIONS

The work documented in this report is intended to provide information about the possible reactivity consequences of fuel reconfiguration during transportation after ES. The approach described above is to generate several scenarios that bound the most likely credible reconfiguration configurations. The results may be useful to guiding research or regulatory approaches to the problems associated with ES.

The results of this work effort are summarized by cask type in this section.

6.1 MPC-24 SUMMARY

The detailed results for each scenario considered in the MPC-24 are provided above in Section 5.1. The results are summarized in Table 4.

The highest reactivity impact involves the preferential flooding of the cask basket in such a way as to moderate the fuel but leave the flux traps dry. The flux traps are an essential feature of the cask, and the basket had been designed to make this preferential flooding scenario extremely unlikely. This scenario is included here to emphasize the importance of maintaining flux trap integrity despite any degradation of fuel, basket, or cask materials that occur during ES.

Assuming the flux traps remain flooded during reconfiguration scenarios, the next most significant reactivity impact comes from the pellet array scenario for gross assembly failure. It is also apparent that maximum axial misalignment is a potentially significant contributor to reactivity increase. Some amount of misalignment is likely to be acceptable, so complete functionality of the assembly spacers is likely not needed subsequent to ES. Material mechanical performance is important to address nonetheless, to ensure maximum misalignment does not occur. The remaining reconfiguration scenarios all have reactivity consequences in the range of 2% Δk_{eff} or less. The addition of three assumptions regarding flux trap condition, cladding performance, and fuel assembly alignment reduces to a manageable level the consequences of the fuel reconfiguration scenarios considered.

6.2 GBC-32

The detailed results for each scenario considered in the GBC-32 are provided above in Section 5.2. The results are summarized in Table 8.

The largest reactivity impact for the GBC-32 cask is the pellet array scenario for gross assembly failure. This scenario is significantly worse than any other scenario considered, including the homogenous rubble case. It demonstrates again the importance of being able to eliminate the consideration of all scenarios involving gross cladding failure in transportation following ES.

Once gross cladding failure has been removed from consideration, the axial misalignment of fuel assemblies is the next most limiting reconfiguration scenario. Both the 20 cm and 30 cm scenarios cause significant reactivity increases because of the high reactivity fuel exposed in the upper portion of the assembly. The axial alignment of burned fuel appears to be more important for maintaining reactivity control within transportation casks after ES than it is for fresh fuel. This result is anticipated given that the reactivity of the fresh fuel is controlled by the center regions of the assembly.

The remaining reconfiguration scenarios all result in reactivity increases of less than 3% Δk_{eff} . This level of reactivity change is manageable. An additional loading curve could be generated to offset the 3% reactivity penalty associated with transportation reconfiguration scenarios. This margin could probably be provided by 8,000–12,000 MWd/MTU of additional burnup or 30 years or more of cooling time beyond the 5 year minimum considered in this work. The very nature of ES lends itself to crediting the extended storage time; it may be possible to demonstrate that no additional restrictions are needed beyond the extended storage time.

6.3 MPC-68

The detailed results for each scenario considered in the MPC-68 are provided in Section 5.3. The results are summarized in Table 20.

The largest reactivity impact for the MPC-68 cask is the pellet array scenario for gross assembly failure. This scenario is significantly worse than any other scenario considered, including the homogenous rubble case. It once again demonstrates the importance of eliminating the consideration of all scenarios involving gross cladding failure in transportation following ES.

Once gross cladding failure has been removed from consideration, the axial misalignment of fuel assemblies is the next most limiting reconfiguration scenario. Both the 20 cm and 38 cm scenarios cause significant reactivity increases because of the high reactivity fuel exposed in the upper portion of the assembly. The axial alignment of burned fuel appears to be very important for maintaining reactivity control within transportation casks after ES.

For the MPC-68 cask, array control is also important. The reactivity consequence of expanded uniform pitch is too large to account for if it cannot be precluded even in the channeled fuel condition. The effort needed to demonstrate that gross cladding failure will not occur following ES should provide a basis for maintaining the assembly array as well. This synergy should be possible because the fuel assembly channel and grids are composed of the same materials as the fuel rod cladding.

It will also be important to demonstrate that large poison defects do not occur uniformly throughout the MPC-68 basket. Fortunately, a large effort is already invested in the demonstration of the long-term viability of cask poison materials. Some of this work is presented in Ref. 21.

The reactivity consequence of the rod removal and minor poison damage scenarios is less than about 3% Δk_{eff} . The margin to mitigate the impact of these scenarios could be provided by an additional loading restriction. The margin should be generated by 15,000 to 20,000 MWd/MTU of additional burnup. Fuel assembly cooling time does not provide sufficient margin to offset these scenarios. The cooling time margin is significantly reduced in BWR fuel because of the extreme axial burnup profile considered and the corresponding low end of life burnups. The fuel composition at these low burnups has significantly less ^{241}Pu and ^{155}Eu than PWR fuel with the same assembly average burnup. The modest inventory of these key isotopes limits the cooling time credit.

6.4 GENERIC CONCLUSIONS

It is possible to draw some generic conclusions that impact all the fuel and cask systems examined as part of this work. The conclusions may be useful to help guide materials research efforts related to ES.

The first conclusion is that material properties characterization regarding structural integrity after ES is a very important parameter to understand regarding reconfiguration scenario development. Each of the three casks examined in this work suffered severe reactivity insertions associated with gross assembly failure. The consequences are too severe to be mitigated with simple technical changes and must therefore be precluded by analysis of the system.

It is possible to conclude that the analysis of additional large-capacity cask designs or additional fuel types is likely to result in different reactivity results, but the important scenarios will be similar. This conclusion is already supported by the similarities in the important effects between PWR and BWR fuel considered in this report. The differences between BWR and PWR fuel designs are more significant than the differences among assembly types within the PWR or BWR fuel classes. The importance of poison damage or fuel assembly alignment will vary from one cask design to another, but the most limiting reconfiguration scenarios will be associated with gross assembly failure and large axial misalignment.

A final conclusion is that specific detailed scenario development is likely to provide significant margin compared to the bounding scenarios considered here. As discussed in Section 4, each of the scenarios

investigated as part of this work was generated with the intent of increasing reactivity in a bounding manner.

7. RECOMMENDATIONS FOR FUTURE WORK

Future work to extend these analyses would be the inclusion of additional fuel assembly types and cask designs. As noted above in Section 6.4, this will not result in significantly different conclusions. It may be beneficial to investigate more accurate modeling of the fuel assemblies to include such features as axial blankets, radial enrichment zoning, and part-length fuel rods. These details could give slightly more realistic estimates of their reactivity impacts but are unlikely to change the salient conclusions regarding the reconfiguration scenarios.

One area in which new or different fuel assembly designs could profitably be considered would be investigating different enrichment and burnups. It is unlikely that the relative importance of scenarios would be impacted by these changes, but the overall magnitude would likely be affected.

A more complete study of degraded fuel forms is also potentially worth investigating. Many degraded fuel forms would include oxidation to other uranium compounds of lower densities, effectively displacing moderator. These changes may not result in any increases in estimated reactivity, however, since none of the scenarios for fuel rubble considered here reached optimum moderation. A low density uranium system would be expected to be farther from peak moderation, but some of these systems might be worth investigating.

More detailed scenario modeling might be considered. More realistic calculations might demonstrate that some of the conditions are incredible.

Some of the scenarios, such as uniform pitch expansion, might be expanded to investigate configurations excluded from these analyses. Two examples are mentioned above in Section 4.3. These include expanding the pitch in the loss of array control cases such that the fuel rods are in contact with the basket and the impact of varying the pitch axially. Fuel assembly sections with a uniformly smaller pitch might prove to be highly effective reflectors for the more reactive sections near the ends with an increased pitch. Additional failure scenarios, such as fuel debris trapped within an intact assembly lattice, could also be considered.

Only one axial burnup and void history is considered in these analyses. A more complete survey of potential histories may be warranted. The results of any such survey are unlikely to generate significant deviations from the results seen here, however. At present, no database of BWR profiles exists that is as extensive as the PWR database of Ref. 20.

Other work should investigate the potential impact of loading varied fuel assemblies in storage casks for ES. These scenarios are more realistic since each assembly experiences different conditions during irradiation. The interaction of different reactivity assemblies may impact the change in calculated k_{eff} values for some scenarios.

The multiple rod removal scenario could be performed stochastically. The random removal of rods would most likely result in a lower and more realistic change in k_{eff} . This study could also vary the rods removed in different assemblies, adding another level of realism to the analysis.

In some cases, it may be advisable to consider combinations of the scenarios used here. The combination of multiple rod removal and rod pitch increase is potentially plausible. A review of other combined effects could generate additional limiting scenarios.

Finally, more work should be performed to identify and quantify mitigating factors to reduce the impact of fuel reconfiguration. The use of additional burnup and cooling time has been discussed in this report, but other mitigation strategies should also be developed.

REFERENCES

1. Title 10, *Code of Federal Regulations*, Part 72, 73 FR 63572, October 24, 2008.
2. Title 10, *Code of Federal Regulations*, Part 71, 73 FR 63572, October 24, 2008.
3. NUREG-1536, Revision 1, *Standard Review Plan for Spent Fuel Dry Storage Systems at a General License Facility*, Office of Nuclear Material Safety and Safeguards, July 2010.
4. NUREG-1567, *Standard Review Plan for Spent Fuel Dry Storage Facilities*, Office of Nuclear Material Safety and Safeguards, March 2000.
5. NUREG-1617, *Standard Review Plan for Transportation Packages for Spent Nuclear Fuel*, Office of Nuclear Material Safety and Safeguards, March 2000.
6. Title 10, *Code of Federal Regulations*, Part 50.68, 71 FR 66648, November 16, 2006.
7. K. R. Elam, J. C. Wagner, and C. V. Parks, *Effects of Fuel Failure on Criticality Safety and Radiation Dose for Spent Fuel Casks*, NUREG/CR-6835 (ORNL/TM-2002/255), prepared for the U.S. Nuclear Regulatory Commission by Oak Ridge National Laboratory, Oak Ridge, Tenn., September 2003.
8. *Safety Analysis Report for the Holtec International Storage, Transport, and Repository Cask System (HI-STAR 100 Cask System)*, Table of Contents to Chapter 1, Holtec Report HI-951251, Revision 10, Holtec International, August 2003, ADAMS Accession Number ML071940386.
9. *Safety Analysis Report for the Holtec International Storage, Transport, and Repository Cask System (HI-STAR 100 Cask System)*, Chapter 2 through Chapter 4, Holtec Report HI-951251, Revision 10, Holtec International, August 2003, ADAMS Accession Number ML071940391.
10. *Safety Analysis Report for the Holtec International Storage, Transport, and Repository Cask System (HI-STAR 100 Cask System)*, Chapter 5 to end, Holtec Report HI-951251, Revision 10, Holtec International, August 2003, ADAMS Accession Number ML071940408.
11. J. C. Wagner, M. D. DeHart, and C. V. Parks, *Recommendations for Addressing Axial Burnup in PWR Burnup Credit Analyses*, NUREG/CR-6801 (ORNL/TM-2001/273), prepared for the U.S. Nuclear Regulatory Commission by Oak Ridge National Laboratory, Oak Ridge, Tenn., March 2003.
12. D. P. Henderson et al., *Summary Report of Commercial Reactor Criticality Data for Quad Cities Unit 2*, B00000000-01717-5705-00096 Revision 01, Civilian Radioactive Waste Management System Management & Operating Contractor, September 1999.

13. D. P. Henderson et al., *Summary Report of Commercial Reactor Criticality Data for LaSalle Unit 1*, B00000000-01717-5705-00138, Civilian Radioactive Waste Management System Management & Operating Contractor, September 1999.
14. *SCALE: A Comprehensive Modeling and Simulation Suite for Nuclear Safety Analysis and Design*, ORNL/TM-2005/39, Version 6.1, Oak Ridge National Laboratory, Oak Ridge, Tennessee, June 2011. Available from Radiation Safety Information Computational Center at Oak Ridge National Laboratory as CCC-785.
15. J. C. Wagner, *Computation Benchmark for Estimation of Reactivity Margin from Fission Products and Minor Actinides in PWR Burnup Credit*, NUREG/CR-6747 (ORNL/TM-2000/306), prepared for the U.S. Nuclear Regulatory Commission by Oak Ridge National Laboratory, Oak Ridge, Tenn., October 2001.
16. C. V. Parks, M. D. DeHart, and J. C. Wagner, *Review and Prioritization of Technical Issues Related to Burnup Credit for LWR Fuel*, NUREG/CR-6665 (ORNL/RM-1999/303), prepared for the U.S. Nuclear Regulatory Commission by Oak Ridge National Laboratory, Oak Ridge, Tenn., February 2000.
17. J. C. Wagner and C. V. Parks, *Recommendations on the Credit for Cooling Time in PWR Burnup Credit Analysis*, NUREG/CR-6781 (ORNL/TM-2001/272), prepared for the U.S. Nuclear Regulatory Commission by Oak Ridge National Laboratory, Oak Ridge, Tenn., January 2003.
18. J. C. Wagner and C. V. Parks, *Parametric Study for the Effect of Burnable Poison Rods for PWR Burnup Credit*, NUREG/CR-6761 (ORNL/TM-2000/373), prepared for the U.S. Nuclear Regulatory Commission by Oak Ridge National Laboratory, Oak Ridge, Tenn., March 2002.
19. C. E. Sanders and J. C. Wagner, *Study of the Effect of Integral Burnable Absorbers for PWR Burnup Credit*, NUREG/CR-6760 (ORNL/TM-2000/321), prepared for the U.S. Nuclear Regulatory Commission by Oak Ridge National Laboratory, Oak Ridge, Tenn., March 2002.
20. R. J. Cacciapouti and S. Van Volkinburg, *Axial Burnup Profile Database for Pressurized Water Reactors*, YAEC-1937, Yankee Atomic Electric Company, May 1997.
21. *Handbook of Neutron Absorber Materials for Spent Nuclear Fuel Transportation and Storage Applications: 2009 edition*, EPRI Technical Report 1019110, Electric Power Research Institute, Palo Alto, California, November 2009.
22. L. B. Wimmer, *BWR Axial Burnup Profile Evaluation*, Framatome ANP Document Number 32-5045751-00, July 16, 2004.